

# Metamorphic Flexure Bearings for Extended Range of Motion

*Dedicated to the memory of Mark Ahearn (1959 - 2024), whose favorite motion picture — a biographical sports car racing drama — would not have been possible without the coordination of hundreds of high-performance mechanical bearings.*

## Cameron R. Taylor<sup>1</sup>

Department of Mechanical and Aerospace Engineering,

University of California Los Angeles, Los Angeles, CA 90095, USA.

Joint Department of Biomedical Engineering,

University of North Carolina at Chapel Hill and North Carolina State University,  
Chapel Hill, NC 27599, USA.

ctaylor7@unc.edu

## Will Flanagan

Department of Mechanical and Aerospace Engineering,

University of California Los Angeles, Los Angeles, CA 90095, USA.

wflan@ucla.edu

## Talmage H. Jones

Department of Mechanical and Aerospace Engineering,

University of California Los Angeles, Los Angeles, CA 90095, USA.

tjones19@ucla.edu

## He Kai Lim

Department of Mechanical and Aerospace Engineering,

University of California Los Angeles, Los Angeles, CA 90095, USA.

limhekai@ucla.edu

## Jonathan B. Hopkins

Department of Mechanical and Aerospace Engineering,

University of California Los Angeles, Los Angeles, CA 90095, USA.

hopkins@seas.ucla.edu

Member, ASME

## Tyler R. Clites<sup>1</sup>

Department of Mechanical and Aerospace Engineering,

University of California Los Angeles, Los Angeles, CA 90095, USA.

clites@ucla.edu

---

<sup>1</sup> Corresponding authors

## ABSTRACT

*Flexure bearings provide precise, low-maintenance operation but have a limited range of motion compared to conventional bearings. Here we introduce a new class of bearing – the metamorphic flexure bearing – that retains the advantages of precision, low wear, and low hysteresis over its limited flexure-bearing range, but also provides an extended range of motion as needed. This extended range of motion is achieved via a position-activated transition to a conventional sliding or rolling bearing. To demonstrate the operating principles of this new class of bearing, we describe, design, assemble, and test a linear-motion metamorphic flexure bearing using three categorically-different transition mechanisms: a compression spring, a constant-force spring, and a pair of magnetic catches. This design paradigm has the potential to provide various benefits (e.g., reduced wear, reduced downtime, cost savings, and increased safety) in areas ranging from precision manufacturing to healthcare robotics to biomedical implants.*

## 1 INTRODUCTION

Mechanical motion has conventionally been guided by surfaces that constrain that motion [1]. Conventional mechanical bearings (i.e., sliding and rolling bearings) enable components to be conveyed over long distances [2], and state-of-the-art conventional mechanical bearings do so with substantially reduced friction compared to their historical counterparts [3]. This reduction in friction results in higher energy efficiency and operational lifetime of the components used in transportation, manufacturing, and household devices [4]. And yet, all bearing surfaces, because they move by rolling, rubbing, or sliding, inevitably have some amount of friction [5], limiting the efficiency of the motion and necessitating maintenance and repair as the mechanisms wear [6].

Flexure bearings offer a frictionless solution to motion control by guiding motion without the use of sliding or rolling contacts [7]. This motion guidance is achieved via compliant flexures that instead bend to convey their components while guiding their motion in a designable way [8]. Because of this designability, flexure bearings can (similarly to conventional bearings) be used for various types of motion, such as linear (e.g., double parallelogram linear bearings) or rotary motion (e.g., cross pivots), or various combinations of such [9,10]. By employing compliant flexures, flexure bearings enable highly repeatable motion with low wear [11], and when optimized for a particular application, they can be designed to outlast the systems in which they are installed [12]. The non-zero stiffness of flexure bearings – in contrast to the zero (or low) stiffness of traditional bearings – is also a benefit in some applications, and this stiffness can be tuned to a desired (even nonlinear) profile as needed for a given application. Further, the low friction of flexure bearings provides for highly efficient, quiet motion that can also be more easily controlled at a higher bandwidth [7]. While other bearing types, such as magnetic or fluid bearings [13], also guide motion without the use of surface contact, they are more often complex, expensive, and difficult to maintain and suffer from inefficiencies such as eddy current or viscous friction losses, and thus are not considered in this paper.

Unfortunately, flexure bearings are also well-known to have a limited range of motion [14]. As many applications require extended ranges of motion, they are thus precluded from the use of flexure bearings and unable to gain the full benefits of using compliant

mechanisms. Hence, mechanical designs would benefit from a bearing design that combines elements of both flexure and conventional bearings. Hybrid bearings do exist that combine flexural elements with sliding, rolling, or interlocking elements, [15–17], but these hybrid bearings have not been designed with the intention of providing an extended range of motion. Thus, we still lack a bearing that provides the advantages of a flexure bearing over a typical range of motion while delivering a larger range when needed.

To address this need, we have developed a new class of bearing – the metamorphic flexure bearing – that functions as a flexure bearing over a small but predominant range of motion and can fully transition to a conventional bearing for intermittent, extended-range use. Importantly, the bearing typically operates in mutually exclusive modes: a flexure-bearing mode and a conventional-bearing mode. In its flexure-bearing mode, it retains all the benefits of a flexure bearing and can be optimized to support a typical loading profile over that range. In its conventional-bearing mode, it acquires a large range of motion while temporarily inheriting the disadvantages of a conventional bearing. Thus, for mechanisms that typically only require a small range of motion (e.g., automotive steering wheels, aviation control yokes, throttle controls), but occasionally require an extended range (e.g., tight turns, high acceleration, hard braking), the metamorphic flexure bearing adds all the benefits of flexure bearings over the small range, high-frequency portions of the mechanism's operation, without restricting its motion over the occasionally required extended range.

In this work, we introduce the concept of the metamorphic flexure bearing and describe its salient principles of operation. We then design, assemble, and characterize a linear-motion bearing demonstrating these operational principles. In our design, we identify and demonstrate three distinct mode-transition strategies, each providing a progressively larger range extension and progressively reduced force profile. We then advance a theoretical framework for the design of a metamorphic flexure bearing, including the selection of a mode-transition strategy, the consideration of device acceleration and velocity, and awareness of the effects of compliance in rigid components. Further, we provide design strategies for bidirectional range extension, and we discuss the implementation of the bearing with other degrees of freedom (e.g., a rotary bearing). This new design framework extends the benefits of compliant mechanisms to a variety of applications that, due to their intermittent need for extended range, until now have been precluded from these benefits.

## 2 THE METAMORPHIC FLEXURE BEARING

### 2.1 Principles of Operation

A metamorphic flexure bearing has at least three rigid bodies: a stage, an intermediate body, and a grounded body (see the top left subfigure of Fig. 1). The stage is connected to the intermediate body via a flexure bearing, and the intermediate body is connected to ground via a conventional bearing (shown in the diagram as a sliding contact).

The bearing has at least two distinct modes of operation: (default) flexure-bearing mode and (intermittent) conventional-bearing mode. In its default mode, the intermediate body is anchored to the grounded body by a retention mechanism so that only the stage is able to move. In this mode, the stage's range of motion limitations are enforced by internal hard stops at the end of its range within the intermediate body. When external force on the stage moves the stage to the end of its range of motion and overcomes the preload of the retention mechanism, the bearing transitions into conventional-bearing mode. In conventional-bearing mode, the intermediate body moves relative to the ground by rolling or sliding. Of note is that the force used to actuate or maintain the bearing position is *only* applied externally to the stage (any forces on the intermediate body are solely internal forces). Movement of the intermediate body is mechanically programmed to occur automatically at the position-dependent transition to conventional-bearing mode, as is re-anchoring of the intermediate body to ground upon re-entering flexure-bearing mode.

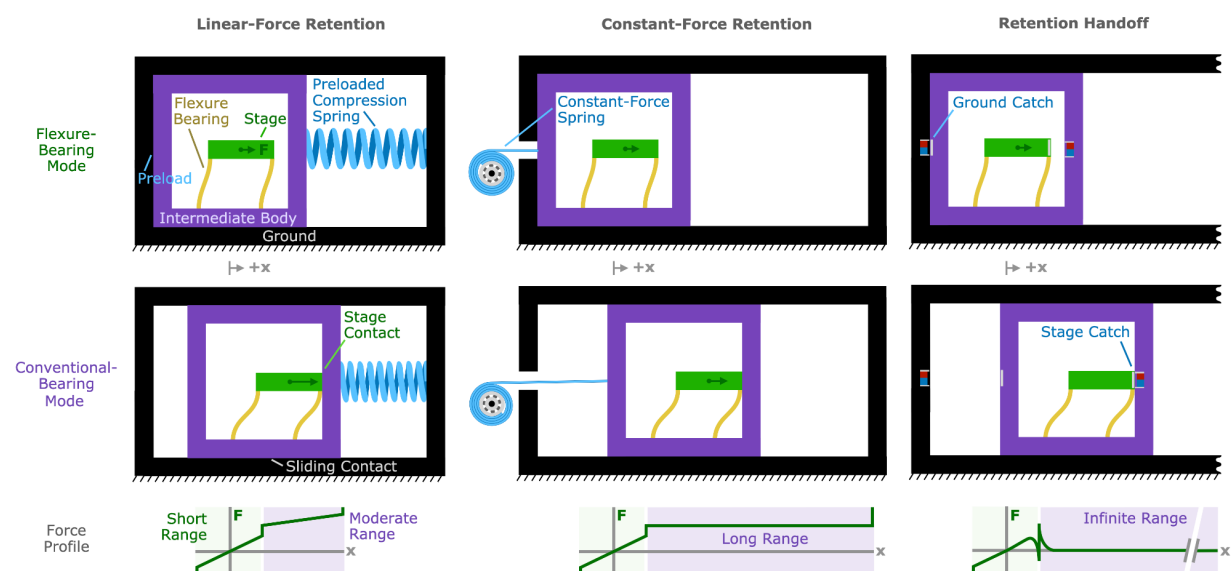


**Fig. 1.** Metamorphic flexure bearings. From left to right, these diagrams describe linear-motion metamorphic flexure bearings that use linear-force retention, constant-force retention, and retention handoff, respectively. The first row shows the bearings in flexure-bearing mode, the second row shows the bearings after transition into their intermittent conventional-bearing mode, and the third row displays the theoretical force profiles corresponding to each retention mechanism, showing the force required to hold the bearing at any given position (with the flexure-bearing range highlighted in green and the conventional-bearing range highlighted in purple). The fixed grounded body (black) has a sliding surface contact to an intermediate body (purple), which is connected to the stage (green) through a linear-motion parallelogram flexure bearing (yellow). In flexure-bearing mode, the preload (labeled with blue text) is maintained by a retention mechanism (blue). Note that on each force profile plot, from left to right, the range of motion increases while the required force on the stage for a given conventional-bearing mode position decreases.

## 2.2 Retention Mechanism Principles

While any device that couples force to motion could feasibly be used to automate the position-dependent transition between flexure-bearing and conventional-bearing mode, we demonstrate just three retention mechanism strategies in this work. Each retention mechanism has a different profile of the force used to actuate the bearing over its mode transition and conventional-bearing range of motion. For all metamorphic flexure bearings, the force is a piecewise function consisting of the flexure-bearing force over

the flexure-bearing range and of the retention mechanism force exerted over the mode transition and conventional-bearing range (plus any hysteretic frictional force due to the conventional bearing). Of note, the force profile over the flexure-bearing range is independent of the retention mechanism type except when the retention mechanism exerts a force near the end of that range. One important design consideration is the amount of force required to overcome the retention mechanism and enter conventional bearing mode. To transition into conventional bearing mode, the external force on the stage must exceed the preload of the intermediate body against the grounded body. Relatedly, for the bearing to stay in flexure-bearing mode until its transition point, the preload provided by the retention mechanism must be tuned to be at least as high as the maximum force of the flexure bearing; otherwise, the bearing will enter a combined mode before reaching the end of the flexure bearing's range of motion. When in this combined mode, both the flexure and conventional bearings are active (and the intermediate body is under-constrained), reducing the range over which the bearing possesses the benefits of solely acting as a flexure bearing.

### *2.2.1 Linear-Force Retention Principles*

Our first retention mechanism is a single preloaded compression spring (see the first column of Fig. 1). A preloaded coil spring with stiffness  $k$  and initial compression  $x$  exhibits a force  $F=kx$  [18]. Thus, when designing a metamorphic flexure bearing with a compression spring retention mechanism, key design considerations include the appropriate spring stiffness  $k$  for the retention mechanism and the necessary initial

compression  $x$ . To maintain the bearing in flexure-bearing mode throughout its full flexure-bearing range of motion, these parameters should be chosen to ensure that the preload  $F$  is above the force required to move the flexure bearing to its range of motion limit.

After the bearing transitions to conventional-bearing mode, further external force on the stage is opposed by the reaction force from the compression spring, which presses the intermediate body against the stage and, consequently, holds the stage's flexures at the end of their compliant range of motion. Thus, with this retention strategy, the same (continuous) retention mechanism anchors the intermediate body to ground during flexure-bearing mode and holds the intermediate body to the stage during conventional-bearing mode, in both cases by exerting an internal force between the ground and the intermediate body. Notably, when considering conventional-bearing mode range extension with a compression spring retention mechanism, another key design consideration is the fully-compressed length of the compression spring relative to its initial preloaded length, because the bearing can only move as far as the compression spring can deform.

### *2.2.2 Constant-Force Retention Principles*

Linear-force retention requires progressively more force to hold the bearing's position the farther it is actuated, but some applications may benefit from a force profile that is constant throughout their range extension. For such designs, a constant-force (c-f)

spring can instead provide the retention force (see the center column of Fig. 1). In this work, we focus on the use of pre-stressed spiral-wound springs, also known as negator springs [19], as constant-force retention mechanisms. To select an appropriate c-f spring, the design engineer need only choose a c-f spring with a force  $F_c$  above the maximum force of the flexure bearing.

In constant-force retention, after the bearing transitions to conventional-bearing mode, all that is needed to maintain the position of the stage at any position throughout the full range of the conventional-bearing mode range of motion is the constant force  $F_c$  to match the c-f spring. This contrasts with the growing force required to access additional range in linear-force retention. Similarly to linear-force retention, however, constant-force retention is a continuous retention mechanism, exerting an internal force throughout the bearing's range.

The range of motion of a metamorphic flexure bearing with this retention mechanism is limited by the maximum extension length of the c-f spring (the point at which one and a half turns of the spring remain on its mounting shaft, in the case of a negator spring). This limit can be accounted for by selecting a c-f spring with a desired fully-extended length, and should be enforced by a hard stop to protect the c-f spring.

### *2.2.3 Retention Handoff Principles*

Some applications may require a particularly far-reaching extended range of motion, or a very low force profile in conventional-bearing mode. Such applications can benefit from transferring (or “handing off”) the intermediate body retention from the grounded body mechanism to the stage mechanism at transition. This allows the design to break free of all range-of-motion limitations imposed by single ground-to-intermediate-body retention mechanisms. We call this concept “retention handoff.” In retention handoff, one retention mechanism anchors the intermediate body to the grounded body during flexure-bearing mode, and a separate retention mechanism anchors the intermediate body to the stage during conventional-bearing mode. During transitions between the modes, the engaged retention mechanism transfers retention of the intermediate body to the previously disengaged retention mechanism before itself disengaging. Thus, only one of the two retention mechanisms is active at once except at the momentary periods when the bearing transitions from flexure-bearing to conventional-bearing mode or vice versa.

In this work, we implemented a retention handoff strategy using magnetic catches (see Fig. 1, right subfigures). The magnetic catch topology we utilized consists of two steel plates separated by one or more parallel magnets with the magnets all oriented in the same direction from one steel plate to the other. An attractive force from this magnetic catch topology occurs when a third steel plate – the armature – is brought close to the two steel plates, and the armature completes a high-permeability path for the magnetic

flux. In designing the retention mechanism, the ground-to-intermediate-body magnetic catch (which we will hereafter refer to as the “ground catch”) must have a holding force that is greater than the maximum force of the flexure bearing.

Unlike with continuous (e.g., linear-force or constant-force) retention, no external force is required to maintain the position of the stage after full transition to conventional bearing mode. Specifically, because retention handoff allows the ground catch to restrict its position-dependent force to within a small region, the mechanism requires no forces to maintain any given position in conventional-bearing mode beyond a short distance.

To enable this zero-force operation, due to the lack of continuous retention force between the intermediate and grounded bodies, an intermediate-body-to-stage retention mechanism (which we will hereafter refer to as the “stage catch”) is required to hold the stage at the end of its flexure-bearing range of motion during conventional bearing mode. This stage catch must also have a holding force greater than the maximum force of the flexure bearing, so that the intermediate body stays anchored to the stage during conventional bearing mode.

When the bearing utilizes retention handoff to transition into conventional-bearing mode, its extended range of motion is no longer limited by the characteristics of the retention mechanism, but solely by the length of the conventional bearing. This allows

the design engineer to implement a substantially longer range extension in a more compact form factor.

### **3 IMPLEMENTATION AND TESTING METHODS**

#### **3.1 Implementation**

To test the metamorphic-flexure-bearing concept, we designed a linear-motion metamorphic flexure bearing with a cylindrical form factor (see Fig. 2), 81 mm in diameter and 238 mm long (including grip fixtures on each side). For ease of design and consistency of testing, we designed and assembled only one prototype into which we incorporated all three retention mechanisms in a manner that would make them selectable and tunable. To maximize the flexure-bearing range of motion, we maximized the flexure lengths by inverting the bearing relative to the design diagrams shown in Fig. 1. Specifically, we placed the conventional bearing on the inside of the mechanism and the flexure bearing on the outside while maintaining all functional relationships between the components (see the cross-section diagram of the bearing in Fig. 2 for details). For the flexure bearing, we used a linear-motion flexure bearing with two pairs of curved blade flexures (see Fig. 2 top center), similar to the parallelogram linear-motion flexure bearing diagrammed above, but in a cylindrical form factor. For the conventional bearing, we used a linear-motion plain bearing composed of two square-profile plain bearings (see Fig. 2 top right). To test different retention mechanisms, we incorporated compression springs, constant-force springs, and magnetic catches, as shown on the bottom of the figure. For a view of all parts used in the assembly, see Fig.

3. For specific details on the assembly process and part numbers used, see Supplementary Section S1 Design and Assembly Details and Supplementary Figs. S1-S4.

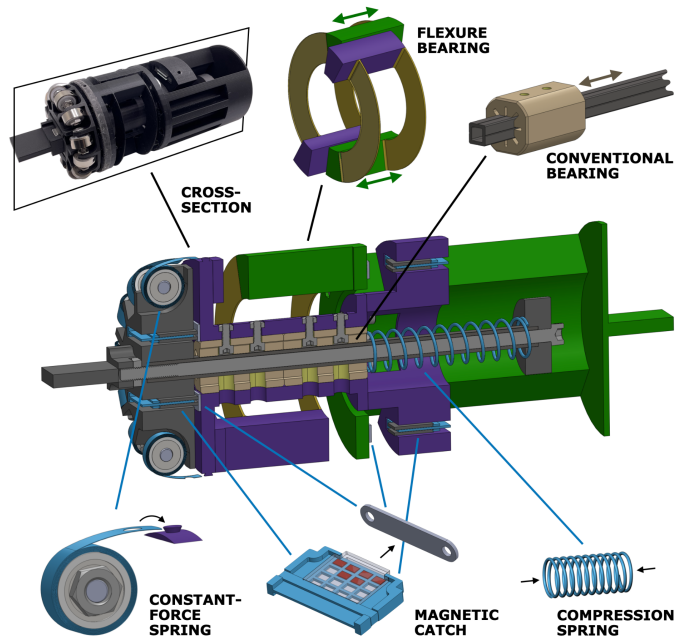


**Fig. 2.** Design of a metamorphic flexure bearing with selectable and tunable retention mechanisms. We designed a cylindrical-form-factor linear-motion metamorphic flexure bearing. The top left image shows the physical bearing, and the center image shows a cross-section view of the design. In the cross-section, the mechanical ground (black) consists of a square linear shaft with two end caps held on by a bolt running through the shaft. The intermediate body (purple) rides on this shaft via two square linear plain bearings (comprising the conventional bearing portion of the mechanism). The intermediate body is connected to the stage (green) through a linear-motion flexure bearing (flexures shown in yellow; attachment rings omitted in detailed view for ease of viewing). The retention mechanisms (all shown in blue) hold the intermediate body to

*the grounded body's home side (left side). Though we used only one retention mechanism at a time during testing, this figure shows all three simultaneously for brevity. To tune the compression spring retention force, we swapped the compression springs for springs of different lengths and fine-tuned initial compression using in-line washers. To tune the constant-force spring retention force, we attached a subset of the constant-force springs to hooks (purple) on the intermediate body. To tune the magnetic catch retention force, we altered the number of parallel, identically-aligned magnets (red) between the steel plates, and we tuned the stage-side magnetic catch in the same manner. Grip fixtures on each end facilitate attachment of the bearing to a universal testing machine for force testing.*

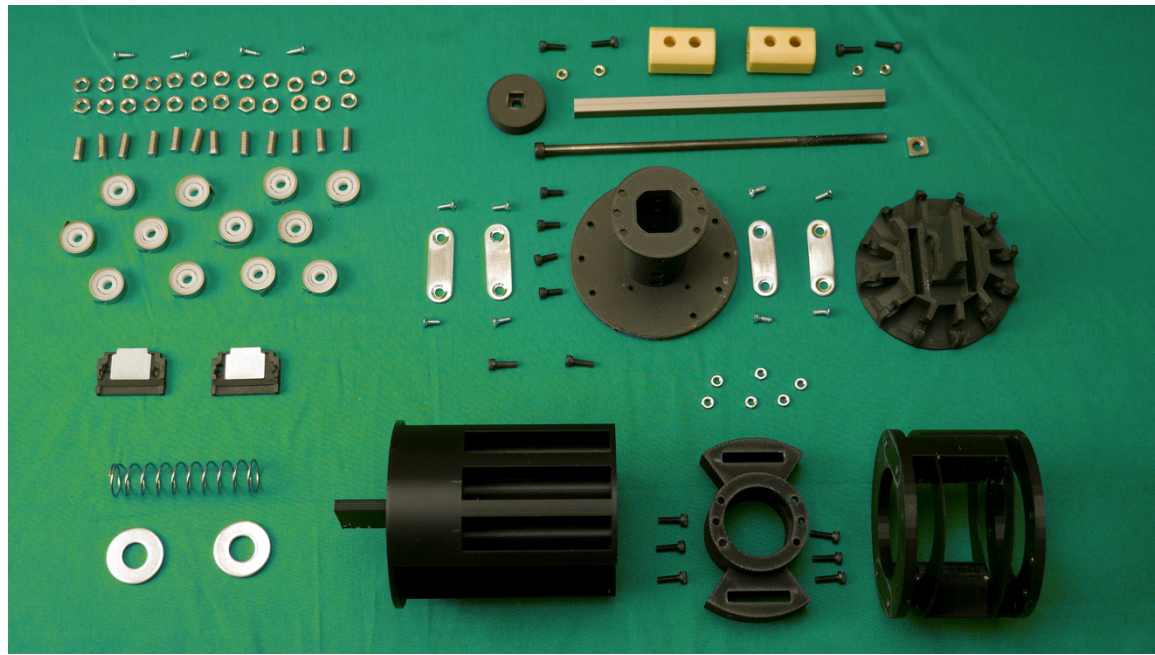


**Fig. 3.** Layout of Parts Used in the Assembly. This figure shows all the parts we used in this work in the implementation of the metamorphic flexure bearing. The retention

*mechanism components are shown at left, the conventional bearing components are shown at top right, and the flexure bearing component is shown at bottom right.*

### **3.2 Experimental Design**

For each of the three retention mechanisms, we characterized the quasi-static force profile of the metamorphic flexure bearing using a universal testing machine (Instron 5966 Dual Column Table Frame). We mounted the bearing vertically into the machine using manual wedge-action grips (Instron 2716-015), with the ground-side grip fixture anchored to the lower grip and the stage-side grip fixture actuated by the upper grip (see Fig. 4). The force required by the upper grip to actuate the bearing was monitored by a load cell installed in series with the upper grip (Instron 2530-500N). Before each test, we tared the load and manually raised the crosshead until it reached a tensile force sufficient to indicate that the far-side hard stop had been reached. Then, we noted the extension value of that hard stop and returned the crosshead to its origin. We then programmed the Instron to shorten the metamorphic flexure bearing until it reached a compressive force of 15 N (indicating the home-side hard stop), lengthen the mechanism to its maximum (far-side hard-stop) extension value, then return the bearing to zero extension, all at a slow speed (10 mm/min) to ensure quasi-static measurements.



**Fig. 4.** Universal machine testing setup for force profile collection. We mounted the bearing vertically between two wedge action grips to measure the quasi-static force throughout its full range. For a time-lapse of a test of the bearing with each of the retention mechanisms, see supplementary Movie S2.

### 3.3 Data Analysis

We removed the first and last two values of collected force data and left the force data unfiltered. For the continuous retention mechanism cases, we used three-point centered finite-difference stencils to compute the first and second derivatives (stiffness and stiffness gradient, respectively) of the force data with respect to extension. We filtered the stiffness using a centered 21-point-window moving average and left the stiffness gradient unfiltered to maintain accurate transition location calculations. We

selected the stiffness filter window length as a trade-off between data clarity and accurate preservation of subthreshold-preload transition locations and stiffnesses. Due to the noisiness and low sampling rate of our data (adaptively varied by the universal testing machine, but approximately 10 Hz in general), we manually selected a tight window for each category within which to programmatically determine transition points.

For the standard continuous retention mechanism cases, we defined the stage attachment and ground detachment as occurring at the stiffness gradient values that were first to exceed 300 N/mm<sup>2</sup> and last to occur below -300 N/mm<sup>2</sup>, respectively, between an extension of 8.5 and 9.5 mm during lengthening (see Figs. S5 and S6 for plots of the stiffness gradients in the continuous retention cases). Similarly, we defined the ground reattachment and stage detachment as occurring at the stiffness gradient values that were first to drop below -300 N/mm<sup>2</sup> and last to remain above 300 N/mm<sup>2</sup>, respectively, between an extension of 9.5 and 8.5 mm during shortening. We calculated each preload as the average between the force at ground detachment and the force at ground reattachment. Finally, we calculated the flexure-bearing range as the average between the extension at stage attachment and the extension at stage detachment, and we averaged corresponding forces at these extensions to calculate the maximum flexure-bearing force. For all curves, range limits were calculated as the first extension value encountered in conventional mode to have a corresponding filtered stiffness value above 1 N/mm.

For the subthreshold-preload continuous mechanism cases, we calculated the ground detachment as occurring at the maximum smoothed stiffness between extension values of 6 and 8 mm in the linear-force case and between 8 and 9 mm in the constant-force case. For the linear-force retention mechanism, we calculated all spring stiffnesses from the unfiltered force curves from extension values of 15 to 40 mm. We then calculated the stage attachment (and detachment) for the linear-force-retention case as the first smoothed stiffness during lengthening (and last smoothed stiffness during shortening) to exceed its corresponding spring stiffness. We used the minimum smoothed stiffness between the ground detachment and stage attachment to report the combined-mode stiffness, averaged with the minimum smooth stiffness between the stage detachment and ground reattachment. We calculated the preload for each subthreshold-preload case as the average between the force at ground detachment and the force at ground reattachment. We then calculated the flexure bearing range as the average of the extension and ground detachment and the extension at ground reattachment.

For the magnetic retention handoff cases, we defined the stage attachment as occurring at the minimum force between 7.5 and 8.5 mm during lengthening and the ground detachment as occurring at the maximum force between 8 and 10 mm during lengthening. We defined the ground reattachment as occurring at the maximum force between 9 and 8 mm during shortening and the stage detachment as occurring at the minimum force between 8.5 and 6.5 mm during shortening. We calculated the weight of

the intermediate body as the average of all curves from 45 to 65 mm, including both the lengthening and shortening phases.

## 4 RESULTS

### 4.1 Characterization

The metamorphic flexure bearing transitioned appropriately with all retention mechanisms tested. Specifically, the bearing automatically transitioned from flexure-bearing mode to and from a conventional-bearing mode at the flexure-bearing range of motion limit in all cases where the retention force was sufficient. We observed a compliant mechanism force profile from approximately -10 to +10 mm (flexure-bearing mode) that was repeatable across all retention mechanism types and retention force levels (see Figs. 5, 6, and 7), with a stiffness proportional to its distance from its zero-force point. We swept through five linear-force, six constant-force, five ground-catch, and five stage-catch preload levels. Each plot below displays the external force required between the ground and stage grip fixtures to quasi-statically hold the bearing at a given extension over the swept preload levels. Range limits at -10 mm and above +45 mm are indicated by dramatically-increasing stiffness. The quasi-static forces of the bearing in the different configurations differed only in the force required for mode transitions and in the forces required during conventional bearing mode (at +10 mm and above).

As expected, hysteresis is observable in the force profiles during conventional-bearing mode due to the friction from the plain bearing. Note that some hysteresis is also

present in the flexure bearing of our prototype due to our use of fused filament fabrication in producing the flexures.

## 4.2 Observed Force Profiles

### 4.2.1 Linear-Force Retention Force Profile

In all five test cases that used linear-force retention, we observed linear force growth throughout the conventional bearing mode (see Fig. 5). We performed one test with each of three compression springs of different lengths and then two additional tests with the shortest spring varying its initial compression and preload using one and then two washers in series. The preloads are labeled for each curve on the force plot, and the transitions and range limits are labeled on the stiffness plot. For the five linear-force retention cases, the measured preloads were 2.1, 4.9, 6.4, 9.7, and 14.5 N, with transitions occurring at approximately 9.1 mm and completing in approximately 0.2 mm in all cases except the 2.1-N preload case. In this case, the transition started at 7.2 mm and finished at 9.6 mm. The difference between these transition cases is illustrated in the figure by the lack of a force step (no stiffness impulse) for the 2.1-N preload case, as well as a momentary drop in stiffness during the transition to 0.348 N/mm (see the figure inset of the stiffness plot in Fig. 5). This 2.1-N preload was below the maximum flexure bearing force of 3.6 N. The spring rates (0.660, 0.662, 0.676, 0.575, 0.492 N/mm) for the five test cases did not substantially differ from their datasheet values. The range limits (varying according to spring initial and maximum compression lengths) were 54.0, 49.7, 48.3, 49.0, and 45.9 mm, with forces at those range limits of 33.5, 32.1, 33.6, 32.8,

and 33.1 N, respectively. See Movie S1 for a demonstration of the metamorphic flexure bearing operation using linear-force retention.

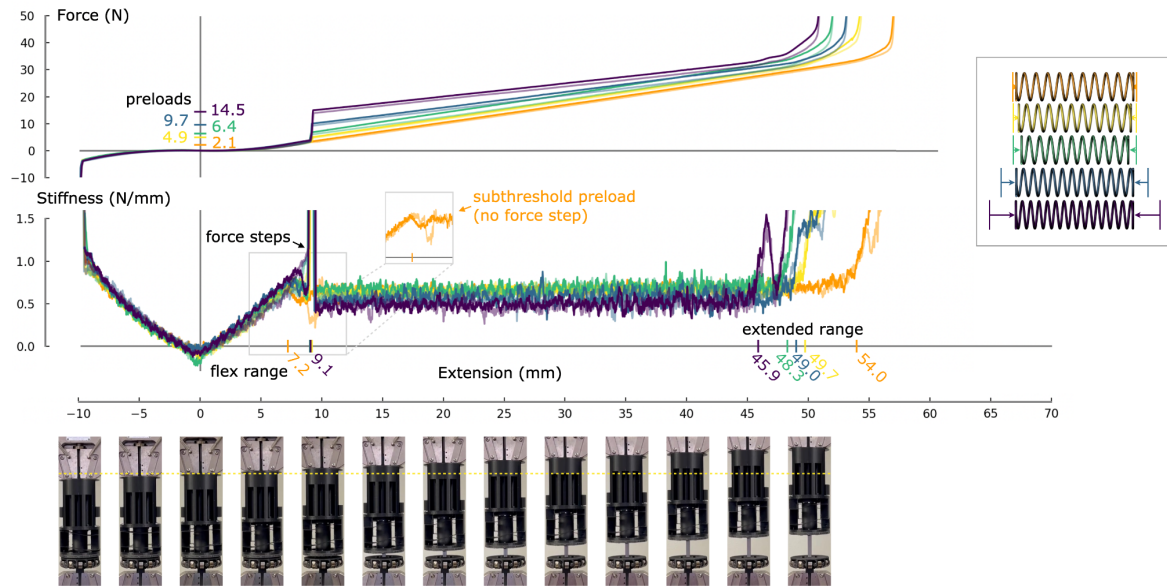


**Fig. 5. Force profile of the metamorphic flexure bearing with linear-force retention.** The force profile of the metamorphic flexure bearing is shown over its full range when using a compression spring for retention. A legend at right shows the compression springs used with vertical bars marking their resting lengths and arrows in corresponding colors indicating the initial compression of the spring during flexure bearing mode, as inserted into the mechanism. Stiffness is also shown, with a shared extension axis (stiffness data smoothed to remove noise). Note that there is a force step at approximately +9.1 mm in all curves except the curve corresponding to the lowest preload level. Images from the Instron test (see Movie S2 for full test) correspond with the extension axis and include a dotted yellow line (colored to match its corresponding force profile curve, the 4.9 N preload case) indicating the equilibrium point. All shortening data are plotted here with

*an alpha value of 0.5 to distinguish them from the lengthening data. See Table 1 for transition data corresponding with this plot.*

**Table 1.** Stage and ground attachment and detachment extensions and forces from linear-force retention force profiles. The extension and force values at the stage attachment, ground detachment, ground reattachment, and stage detachment are shown, with colors corresponding to the plot colors used in Figure 5. Forces are provided in bold for ease of comparison with one another, and the preload forces are italicized for ease of reference. The highlighted values in colors corresponding to plot colors were averaged for plot labeling. The values highlighted in gray show the flexure bearing range and maximum flexure bearing force. The unhighlighted values correspond to transition completion in the subthreshold-preload case. In this case, a combined mode is entered, so the ground detachment occurs before the stage attachment, and the stage detachment occurs before the ground reattachment. This combined mode ends at an extension (shown in red font) beyond the flexure bearing range but at approximately the maximum flexure bearing force.

Stage Attachment		Ground Detachment		Ground Reattachment		Stage Detachment	
Ext (mm)	Force (N)	Ext (mm)	Force (N)	Ext (mm)	Force (N)	Ext (mm)	Force (N)
9.3	<b>3.5</b>	7.0	<b>2.1</b>	7.4	<b>2.1</b>	9.8	<b>3.4</b>
9.2	<b>3.5</b>	9.3	<b>5.1</b>	9.3	<b>4.8</b>	9.2	<b>3.2</b>
9.0	<b>3.5</b>	9.2	<b>6.8</b>	9.2	<b>6.0</b>	9.0	<b>3.1</b>
9.0	<b>3.8</b>	9.2	<b>10.1</b>	9.2	<b>9.3</b>	9.1	<b>3.4</b>
9.1	<b>3.9</b>	9.3	<b>15.1</b>	9.3	<b>14.0</b>	9.1	<b>3.4</b>

#### *4.2.2 Constant-Force Retention Force Profile*

In each of the six test cases that used constant-force retention, we observed that the force remained substantially constant throughout its conventional bearing mode (see Fig. 6). These test cases consisted of retention mechanisms composed of two to twelve constant-force springs in increments of two. The preloads are labeled for each curve on the force plot, and the transitions and range limits are labeled on the stiffness plot. For the six constant-force retention cases, the measured preloads were 2.8, 4.6, 6.5, 8.3, 10.1, and 11.9 N, with transitions occurring at 9.1 mm for all cases except the 2.8-N preload case, in which case the transition started at 8.3 mm and never fully completed the transition into conventional-bearing mode. As in the linear-force retention case, the lack of a force step (and corresponding lack of a stiffness impulse) sets the 2.8-N constant-force case apart from the higher-force cases. This 2.8-N preload was below the maximum flexure bearing force of 3.6 N. The effect of the far-side hard stop was observed at approximately 69.7 mm in all cases, with forces at those range limits of 3.6, 5.4, 7.5, 9.5, 11.6, 13.9 N, respectively, with force increases localized near the beginning of the conventional bearing range (note the relatively small differences between these forces and the preload forces).

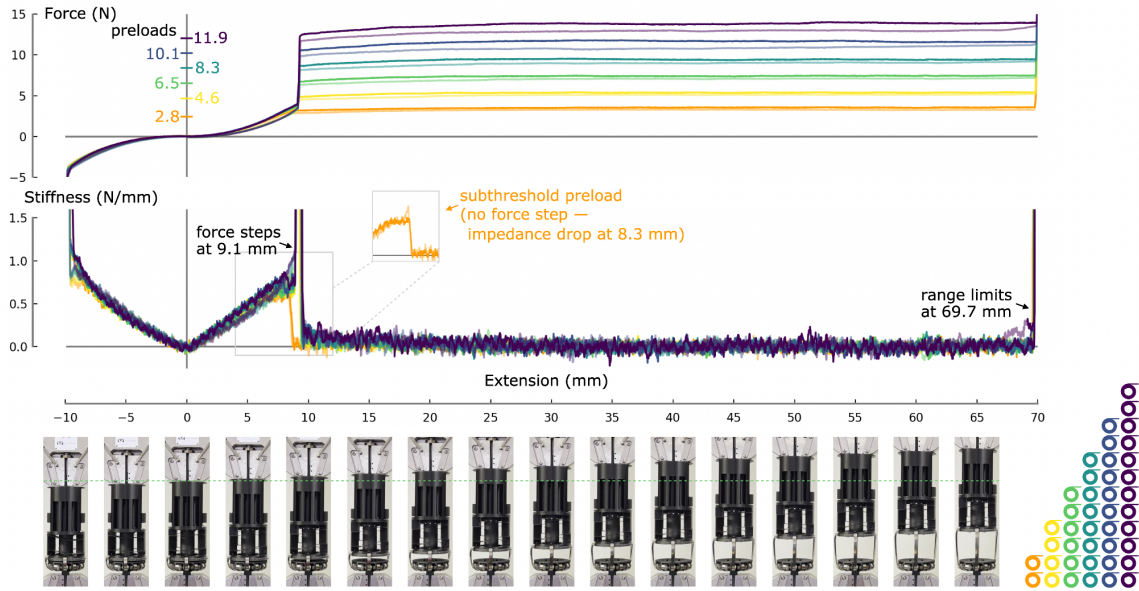


**Fig. 6. Force profile of the metamorphic flexure bearing with constant-force retention.**

The force profile of the metamorphic flexure bearing is shown over its full range when using constant-force springs for retention. The legend in the bottom right corner of the figure shows the number of constant-force springs used in each case. Stiffness is also shown, with a shared extension axis (data smoothed to remove noise). Note the force step at approximately +9.1 mm in all curves except the curve corresponding to the lowest preload level. Due to the constant-force nature of this retention mechanism, the lowest constant-force spring never fully enters conventional-bearing mode, but stays in a combined mode after transition (the stage never contacts the intermediate body). Images from the Instron test (see Movie S2 for full test) correspond with the extension axis and include a dotted light green line (colored to match its corresponding force profile curve, the 6.5-N preload case) indicating the equilibrium point. All shortening

*data are plotted here with an alpha value of 0.5 to distinguish them from the lengthening data. See Table 2 for transition data corresponding with this plot.*

**Table 2.** Stage and ground attachment and detachment extensions and forces from constant-force retention force profiles. The extension and force values at the stage attachment, ground detachment, ground reattachment, and stage detachment are shown, with colors corresponding to the plot colors used in Fig. 6. Forces are provided in bold for ease of comparison with one another, and the preload forces are italicized for ease of reference. The highlighted values in colors corresponding to plot colors were averaged for plot labeling. The values highlighted in gray show the flexure bearing range and maximum flexure bearing force. Note that the stage attachment and stage detachment are intentionally left blank; in the case of constant-force retention, bearings with subthreshold preloads do not complete the transition. Instead, a combined mode is entered into at ground detachment, and the bearing remains in this combined mode until ground reattachment (re-entry into flexure-bearing mode).

Stage Attachment		Ground Detachment		Ground Reattachment		Stage Detachment	
Ext (mm)	Force (N)	Ext (mm)	Force (N)	Ext (mm)	Force (N)	Ext (mm)	Force (N)
9.1	<b>3.6</b>	8.2	<b>2.9</b>	8.3	<b>2.7</b>	9.1	<b>3.3</b>
9.1	<b>3.8</b>	9.1	<b>4.6</b>	9.2	<b>4.5</b>	9.1	<b>3.3</b>
9.1	<b>3.9</b>	9.2	<b>6.7</b>	9.3	<b>6.3</b>	9.1	<b>3.4</b>
9.1	<b>4.1</b>	9.3	<b>8.6</b>	9.3	<b>8.1</b>	9.2	<b>3.5</b>
9.1	<b>4.0</b>	9.3	<b>10.4</b>	9.3	<b>9.8</b>	9.2	<b>3.5</b>
		9.3	<b>12.2</b>	9.4	<b>11.7</b>		

#### *4.2.3 Retention Handoff Force Profile*

In all nine test cases that used retention handoff, we observed a force that remained substantially constant throughout the conventional bearing mode and that was nearly identical across all test cases (see the intermediate body weight zoom inset of the bottom plot in Fig. 7). This force offset was due to gravitational force on the intermediate body that assisted all retention mechanisms, and it would not have been present if the bearing had been oriented horizontally. Rather, this force arose from the positive vertical orientation in which we placed the bearing in the universal testing machine, and was also present (though not obviously so) in the continuous retention mechanism test cases above. For a notes on gravitational retention, see subsection S4.2 on Gravitational Retention.

The nine test cases consisted of five cases sweeping from two to ten magnets in the ground-catch in increments of two while holding the stage-catch force constant, and vice versa. Ground-catch and stage-catch preloads – corresponding to ground detachment and stage detachment, respectively – are labeled for each curve of each sweep in the figure. The stage and ground attachment and separation locations and forces are provided in Table 3.

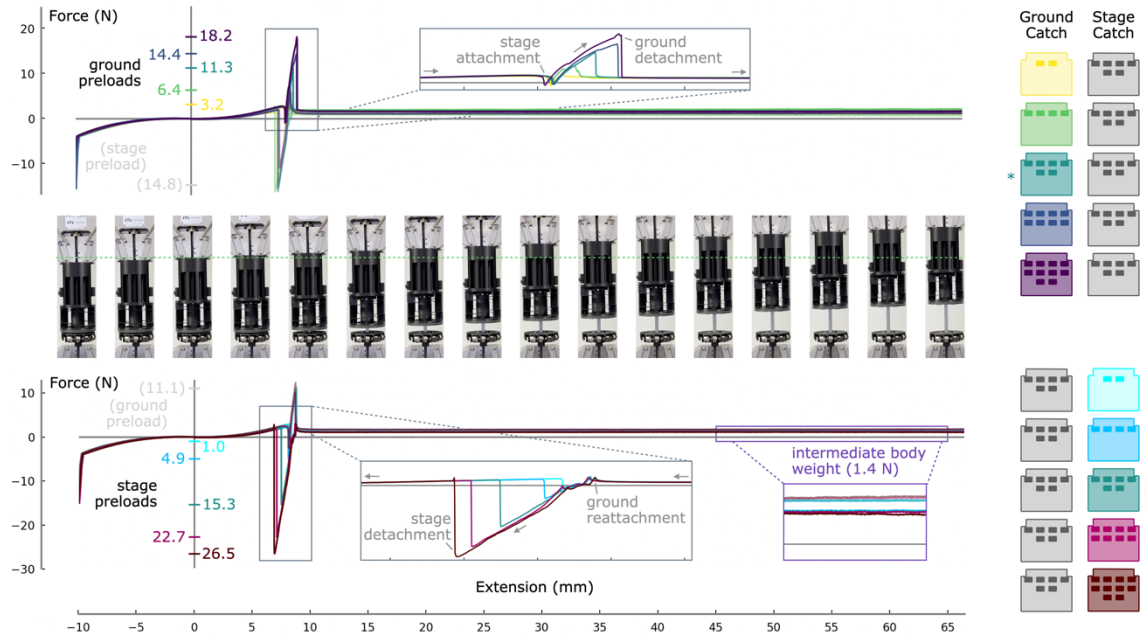


**Fig. 7. Force profile of the metamorphic flexure bearing using retention handoff.** The force profile of the metamorphic flexure bearing is shown over its full range when using magnetic catches for retention. The number of magnets used in the ground catch and stage catch for each case is shown at right, with the colors of the swept-force catch corresponding to the colors of each curve and with an asterisk indicating data that is shown in both plots. The plot above the test images (from Movie S2) shows the extension and return curves for a sweep of ground-catch contact forces at a constant stage-catch contact force, and the plot below shows the extension and return curves for a sweep of stage-catch contact forces at a constant ground-catch contact force. Insets show detail of the swept preload values at the ground and stage detachments. For alternative zoomed-in insets showing changes in attachment forces, see Fig. S7. As noted above, gravitational retention assisted the system in the particular mounted orientation used (for more on gravitational retention, see subsection S4.2 Gravitational Retention).

*Images from the four-magnet-ground-catch six-magnet-stage-catch case Instron test correspond with the extension axis and include a dotted light green line indicating the equilibrium point. The constant-detachment-force data curves are plotted with an alpha value of 0.5 to distinguish them from the detachment-force swept curves. The direction of travel is indicated in the zoom insets with gray arrows. See Table 3 directly below for transition data corresponding with the plots.*

**Table 3.** Stage and ground attachment and detachment extensions and forces for both force profile sweeps. The extension and force values at the stage attachment, ground detachment, ground reattachment, and stage detachment are shown, with colors corresponding to the plot colors used in Fig. 7, and with boxes around values corresponding to the plot zoom insets of Fig. 7 (see Fig. S7 for zoom insets corresponding to the non-boxed values). Forces are provided in bold for ease of comparison with one another, and the preload forces are also italicized for ease of reference. Note that the preload forces correspond to detachments and that the attachment forces are substantially lower in magnitude than detachment forces (for an explanation of this phenomenon, see the Discussion Section Magnetic Catch Asymmetry).

Stage Attachment		Ground Detachment		Ground Reattachment		Stage Detachment	
Ext (mm)	Force (N)	Ext (mm)	Force (N)	Ext (mm)	Force (N)	Ext (mm)	Force (N)
8.2	<b>-1.2</b>	8.3	<b>3.2</b>	8.7	<b>1.4</b>	7.4	<b>-15.2</b>
8.2	<b>0.5</b>	8.5	<b>6.4</b>	8.5	<b>2.3</b>	7.2	<b>-16.2</b>
8.2	<b>-0.7</b>	8.8	<b>11.3</b>	8.7	<b>3.2</b>	7.5	<b>-15.3</b>
8.2	<b>-0.6</b>	9.1	<b>14.4</b>	8.6	<b>5.9</b>	7.5	<b>-16.1</b>
8.1	<b>-0.9</b>	9.1	<b>18.2</b>	8.5	<b>6.9</b>	7.6	<b>-10.9</b>
8.4	<b>2.5</b>	8.8	<b>11.0</b>	8.7	<b>3.1</b>	8.4	<b>-1.0</b>
8.3	<b>0.8</b>	8.7	<b>10.6</b>	8.8	<b>3.0</b>	8.1	<b>-4.9</b>
8.2	<b>-0.7</b>	8.8	<b>11.3</b>	8.7	<b>3.2</b>	7.5	<b>-15.3</b>
8.2	<b>-2.5</b>	8.7	<b>10.2</b>	8.7	<b>3.0</b>	7.1	<b>-22.7</b>
8.1	<b>-2.5</b>	8.7	<b>12.3</b>	8.8	<b>2.9</b>	6.9	<b>-26.5</b>

When approaching the transition from flexure-bearing to conventional-bearing mode, the stage-side magnetic catch (“stage catch”) began to exert an attractive force between the stage and the intermediate body. This internal force reduced the external force required to extend the flexure bearing, typically even requiring an opposing (negative) force just before attachment (see Fig. 7 top zoom inset). After attachment of the stage catch, the force then grew rapidly toward detachment of the ground-side magnetic catch (“ground catch”).

During detachment of the ground catch (see Fig. 7 top zoom inset), the force increased to the full magnetic-catch contact force (which was greater than the maximum flexure bearing force plus the intermediate body weight in all cases tested), then dropped to the intermediate body weight upon transition into conventional-bearing mode.

During re-attachment of the ground catch (see Fig. 7 bottom zoom inset), the catch attached with less required external force between the ground and stage than was needed during detachment (for comparison, refer to the matched-color force profiles in the insets, as indicated by an asterisk in the figure legend). The force then momentarily returned to zero (because the intermediate body weight was again borne by the grounded body) before again building (downward) towards detachment from the stage catch.

During detachment of the stage catch (see Fig. 7 bottom zoom inset), as with the ground catch, the catch required more force to detach than it required during attachment.

We typically found that disengaging a magnetic catch required more travel and force than engaging it. Stronger magnetic catch forces amplified this effect, and it was particularly evident in the stage catch, which was mounted to a less rigid component (the far side of the intermediate-body) than the grounded body. See the Discussion Section Magnetic Catch Asymmetry for an in-depth discussion of this effect.

## 5 DISCUSSION

In this work, we have successfully demonstrated operation of the metamorphic flexure bearing. Over a selected range of motion, the bearing operates as a compliant mechanism (flexure-bearing mode). Beyond this initial limited range, the metamorphic bearing automatically transitions to a conventional mechanism to achieve an extended range (conventional-bearing mode). By defaulting to its flexure-bearing mode over a selected range, this bearing prioritizes the advantages of a flexure bearing up until an extended range is required, at which point it temporarily inherits all the advantages and disadvantages of a conventional bearing.

An important characteristic of the metamorphic flexure bearing is how it handles bearing loads – that is, loads exerted in directions *other* than the bearing's degrees of freedom. With this architecture, bearing loads borne by the conventional bearing will

also be borne by the flexure bearing and vice versa. In other words, all bearing loads are borne in series across the two internal bearings. If the conventional bearing off-axis stiffness is high, the total off-axis stiffness is predominately driven by the off-axis stiffness of the flexure bearing. In applications requiring minimal off-axis movement, flexure topologies or arrangements known to have a higher off-axis to axial stiffness ratio may be more desirable to better control the bearing's motion. In conventional-bearing mode, the flexure bearing sustains bearing loads at its maximum extension. Thus, the flexure bearing should be designed to match the highest load capacity of the bearing, but it need only sustain these loads over its selected range of motion. (Of note, bearing loads borne by a stage-catch retention mechanism reduce the bearing load seen by the flexure bearing.) Consequently, this design makes it possible for some typically low-range applications, for which flexure bearings were not previously suitable, to use flexure bearings with tuned range limits without compromising full extension of the bearing. This new design space enables these applications, which were previously unable to use compliant mechanisms, to now claim the advantages of a flexure bearing – high repeatability, low wear, and low friction – over a selected range.

We implemented and characterized the metamorphic flexure bearing using three example retention mechanisms (linear-force retention, constant-force retention, and retention handoff) and illustrated distinct advantages and disadvantages of each mechanism in the bearing design. In this section, we will first discuss various design principles that we learned by implementing and testing the metamorphic flexure

bearing and by implementing and characterizing these three retention mechanisms. We will then explore other possible retention mechanisms that could be used. Finally, we will generalize the design space of the metamorphic flexure bearing to multiple directions of range extension and to various degrees of freedom and discuss the numerous applications of the metamorphic flexure bearing.

## 5.1 Design Principles

### 5.1.1 Ranges of Motion

The bearing we demonstrated here had a flexure-bearing range of motion of approximately -10 mm to +10 mm and a range extension of 35 mm or more, depending on the retention mechanism and retention mechanism parameters.

In the case of the linear-force retention mechanism, which demonstrated a moderate length range extension, the range extension was limited by abutment against the fully compressed spring. While it would be possible to make this range extension substantially longer by using a considerably longer compression spring, the further range extension would come at the cost of needing to extend the length of the mechanism itself by additional unused length to accommodate the longer fully-compressed spring length. In addition, longer compression springs of a given diameter are less stable against lateral buckling, making it more difficult to find as off-the-shelf components for a longer range extension with linear-force retention.

The constant-force retention mechanism provided a full 60 mm of range extension, but this did not fully demonstrate the potential for range extension with a constant-force (c-f) spring. In reality, the c-f springs we used were capable of a 457 mm maximum extension, permitting a design with a substantially longer conventional-bearing shaft to take advantage of this full length. It is also worthy to note that negator springs have a very limited lifetime – the negator springs we used were rated for just 25,000 cycles. The use of a short-life retention mechanism such as the one we used here has the potential to counteract the longevity benefits of a flexure bearing if the flexure bearing is being optimized for low fatigue but the application requires more than just occasional use of the conventional-bearing-mode range.

While our demonstration of the retention handoff mechanism was limited by the 70-mm hard stop in our design, in practice the bearing need not see a limit on its range of motion under retention handoff. For instance, using retention handoff with a trackless wheeled mechanism (e.g., a cart on a horizontal surface) in a metamorphic flexure bearing would provide an infinite range extension.

### *5.1.2 Force Profile Design*

The variety of possible retention mechanisms with which the metamorphic flexure bearing can be constructed equips the design engineer with the ability to tune the force, and consequently, the stiffness, of the bearing across its full range of motion. For instance, if a constant-stiffness flexure bearing and a linear-force retention mechanism

of the same stiffness are used in the bearing, with the preload equal to the maximum flexure bearing force, the bearing will have a constant-stiffness profile over its full range of motion. This bearing would behave similarly to a constant-stiffness spring and the force profile would provide no indication of when the transition occurs. If, on the other hand, an indication of transitions is desired, a large force step or change in stiffness can be designed into the mechanism. The various curves shown in Figs. 5 and 6 demonstrate this designability and suggest the possibilities of many other force profiles.

Creating characteristically different profiles, however, requires using different retention mechanisms. For instance, of the retention mechanisms we explored here, the retention handoff strategy is the only one we explored that can provide zero-force position maintenance once fully in its conventional bearing mode, mimicking the operation of a typical conventional bearing. There's a point far enough from the ground-side magnetic catch where the magnetic force fades, and the machine's retention mechanism effects just disappear, and all that's left is the stage moving through space as a conventional bearing. It should be noted, however, that, as we observed, the conventional bearing exhibits hysteresis due to friction, an unavoidable limitation of the conventional bearing, which introduces a small amount of force opposing any movement of the bearing while in conventional-bearing mode.

We note that the flexure bearing we used in our experiments itself had a nonlinear force profile and that it is not necessary (nor desirable in all applications) for the flexure

bearing force profile to be linear. In particular, in our implementation, we prioritized minimizing parasitic translation over linearity. In fact, the flexure bearing can have any force profile desired (via different boundary conditions, topologies, geometries, materials, and so on) and still be designed to interact appropriately with a given retention mechanism so long as the retention mechanism's force is sufficient.

#### *5.1.3 Combined-Mode Operation and Maximum Negative Acceleration*

We previously discussed the need to tune the retention mechanism so that its force is greater than the maximum flexure bearing force. However, what happens when this retention force requirement is violated?

Suppose the retention force between the grounded and intermediate bodies is below the maximum flexure bearing force. In this configuration, the intermediate body will disconnect from the grounded body before the stage has contacted the intermediate body, causing the bearing to enter a combined (flexure-bearing and conventional-bearing) mode. The amount of range allocated to this mode should typically be minimized, because any range allocated to the combined mode reappropriates range from the flexure-bearing mode.

Different retention mechanisms interact with combined-mode operation in distinct ways. In the case of linear-force retention, the combined mode is transient and (quasi-statically) repeatable, because the retention mechanism force grows with the range and

will eventually exceed the maximum flexure bearing force. In the case of constant-force retention, any combined mode entered into at transition is persistent, because the retention force (being constant) will never grow to exceed the maximum flexure-bearing force. When using retention handoff, if the ground catch has insufficient force, it will likewise enter a combined mode with an under-constrained intermediate body instead of fully transitioning to conventional-bearing mode. This transition into combined mode under incomplete retention handoff will also result in oscillation of the intermediate body mass due to a jump discontinuity in its quasi-static resting position. Further yet, in the retention handoff case, quasi-static transition from combined mode back to flexure-bearing mode only occurs when the stage fully returns to its home position (unless it has first transitioned into conventional-bearing mode by fully extending to the far-side grounded-body hard stop), increasing the amount of distance traveled in conventional-bearing mode.

Though entering a combined mode at transition is generally undesirable, there may be instances where a combined mode is advantageous. For example, because a combined mode under linear-force retention is transient and repeatable, it guarantees a continuous monotonically-increasing force profile. This could enable the position of the stage to be sensed via the force on the bearing, allowing the bearing to be smoothly positioned-controlled via force control. (For another instance describing a possible advantage of allowing a combined mode, see subsection S4.4 on Conditional Retention.) It should be noted, however, that when in combined mode, the bearing exhibits

reduced stiffness in the linear-force retention case (and zero stiffness in the constant-force case) due to the series arrangement of the flexure bearing and retention spring. In the subthreshold preload case that we tested with linear-force retention, we observed, as expected, a reduction to approximately half stiffness during the combined mode, due to the flexure bearing and retention springs being approximately matched in stiffness, making their effective series-combined spring constant one half their individual stiffnesses.

Venturing beyond quasi-static analysis reveals yet another way for the bearing to enter combined mode. Acceleration of the intermediate body mass requires additional force, which affects the preload between the intermediate body and the stage. While positive acceleration of the stage (relative to the grounded body) increases the contact force between the intermediate body and the stage, negative acceleration (decreasing positive velocity or increasing negative velocity) *decreases* this contact force. Thus, if the force required for negative acceleration of the stage mass exceeds the quasi-static contact force (the difference between the maximum flexure bearing force and the retention force between the intermediate body and the stage), the retention force will be insufficient to accelerate the intermediate body, resulting in the stage disconnecting and the bearing entering combined mode. In the linear-force retention case, the maximum negative acceleration that the bearing can have without entering combined mode grows with increasing positive position of the bearing. In the constant-force retention case, the maximum negative acceleration that the bearing can have without

entering combined mode is constant. In either case, however, the bearing will automatically return to its conventional-bearing mode if the bearing is in its conventional-mode region and the stage ceases to exceed this maximum negative acceleration threshold, because during an acceleration-induced combined mode, the intermediate body is being accelerated at its maximum acceleration, so it will eventually catch up to the stage. On the other hand, when using a retention handoff strategy, any combined mode due to acceleration is again persistent, just as in the case of quasi-static combined-mode entry. Notably, however, in the case of retention handoff, the acceleration threshold can be made different from the quasi-static transition by tuning the stage catch force to be different from the ground-catch force. Further, while we have discussed only inertial forces and assumed ideal conventional bearings and ideal retention mechanisms here, in all these cases, friction and tolerances should also be accounted for in maximum acceleration calculations. Importantly, the maximum acceleration of the stage relative to a fixed ground is a factor to consider in the design of a metamorphic flexure bearing. For notes about operation of the bearing without a fixed ground, see Section S2 Grounded Body Acceleration.

#### *5.1.4 Orientation and Momentum Considerations*

While the bearing need not be in any particular orientation for its operation, if the intermediate body is of non-negligible mass, the weight of the intermediate body will detectably alter the force required to maintain the bearing's position during conventional-bearing mode when the bearing is in any non-horizontal position in an

inertial reference frame (e.g., on earth). In the vertical position in which we mounted the bearing, when taring the load, the weight of the *stage* weight was compensated for. However, upon transition to conventional-bearing mode, the *intermediate-body* weight was added to the weight of the stage and was thus borne by the load sensor, resulting in a corresponding positive increase in the force reading. If we had mounted the bearing upside down (anchoring the stage side to the lower grip and actuating the ground side using the upper grip), when taring the load, the force from the combined grounded and intermediate bodies would have been compensated for. Upon transition to conventional-bearing mode, the intermediate-body weight would have then been removed from the grounded body and thus no longer borne by the load sensor, resulting in a *decrease* in the force reading corresponding to the weight of the intermediate body. Therefore, the effect of intermediate-body weight on the required force to maintain the bearing position, and particularly its effect on preload levels, should be considered when the intermediate-body mass is non-negligible. This effect is related to our discussion above about the simultaneous acceleration of the stage and ground (considering vertical orientation as resulting in gravitational acceleration). Thus, in considering both the acceleration and orientation of the bearing, the intermediate body should generally be designed to have as low a mass as possible while still keeping it a rigid body.

The mass of the stage may also be an important factor for some applications when considering system dynamics. In particular, momentum could be used to smooth out

transitions in the retention handoff case. For instance, when quickly transitioning from flexure-bearing to conventional-bearing mode, the momentum of the stage would be transferred to the combined intermediate body and stage, and this momentum could be sufficient to overcome the ground-side retention mechanism force without any additional force on the stage. In the opposite direction (when quickly transitioning from conventional-bearing to flexure-bearing mode), the momentum of the stage could also be sufficient to overcome the force of the intermediate-body retention mechanism.

#### *5.1.5 Magnetic Catch Asymmetry*

Whenever a magnetic retention mechanism is attached to a compliant component, the compliant component will need to be stretched to the full contact force of the magnetic retention mechanism before detachment occurs, making detachment occur at full force but at a further distance away from the retention mechanism than would be expected with fully-rigid components. Conversely, upon approaching contact, the compliant component will not begin to stretch until the magnetic retention mechanism is close to contacting, and hence, the attachment will occur at a lower force and at a shorter distance from the contact point than the force and distance required for detachment.

See Section S3 Magnetic Catch Asymmetry Model and the corresponding Fig. S8 for further notes on this principle. Because our “rigid” components were composed of plastic, all these components had some non-negligible compliance to them. The effects of this compliance can be seen in the differences between the detachment and attachment forces and locations of our magnetic catches for both the ground catch and

stage catch, and is more clearly observed when the catches are tuned to have higher contact forces. This rigid body compliance is also responsible for the smooth transitions observed with the continuous retention mechanisms, albeit with different stiffnesses for each, determined by the force path through the bearing and by differing application locations of the internal retention-mechanism forces. Notably, the difference between the detachment and attachment forces and positions is substantially larger for the stage catch, where we designed the catch into the mechanism in a location with substantially higher flexion (far from the center axis of the bearing and mounted on an unsupported arm [see Fig. 2]) than the location of the grounded body (close to the center axis of the bearing).

## 5.2 Design Variations

### 5.2.1 Retention Mechanisms

We have shown three possible retention mechanisms here, but there is a vast design space of strategies that can maintain the preload of the intermediate body to the ground and stage in flexure-bearing and conventional-bearing mode, respectively. For example, linear-force retention can be performed with an extension spring instead of a compression spring, or different continuous retention mechanisms can be used (including mechanisms not involving springs) to provide custom force profiles. Even gravitational force can be used as a retention mechanism, which can be implemented using a vertical orientation and a high intermediate body mass, (see subsection S4.2 on gravitational retention). And a variety of other force profiles are also possible. We note

that the slight increase in force we observed in our implementation of constant-force retention agrees with the literature, which describes negator springs as approaching their constant force asymptotically [20]. This can be mitigated by using one of many other possible truly-constant-force mechanisms [21–23]. And finally, while retention handoff can be implemented by a variety of magnetic catch topologies for a variety of force profiles [24], retention handoff need not use magnetic elements; it can be enabled by other catches, such as touch fasteners [25] or roller catches. And for some applications, there may only be a need for a single, ground-side retention mechanism. Detailed notes on other retention mechanism types can be found in Section S4, Further Exploration of Possible Retention Mechanisms.

### *5.2.2 Bidirectional Range Extension*

Although extending the range of a flexure bearing in a single direction can benefit many applications, many other applications require bidirectional range extension (e.g., automotive steering wheels, aviation control yokes, control valves, etc.). In all discussion up to this point, however, we have discussed only range extension beyond one side of the flexure bearing's range of motion, with a hard stop at the other end of its range of motion that denies further movement of the intermediate body in that direction. This hard stop is one way to anchor the intermediate body during flexure-bearing mode, but it also intrinsically prevents bidirectional range extension via the intermediate body. We'll now discuss principles for how intermediate body anchoring can be maintained in

flexure-bearing mode while enabling bidirectional motion via conventional-bearing mode.

Just as a flexure bearing with two internal hard stops can be extended in one direction using a conventional bearing, that conventional bearing with its own two internal hard stops can be extended in the *opposite* direction using *another* conventional bearing.

This design concept is illustrated in Fig. 8, wherein the original grounded body (shown in black) now acts as a second intermediate body that is anchored to a new grounded body (shown in dark blue) via an additional retention mechanism (in this case, a compression spring). When sufficient force is exerted in the direction previously limited by the hard stop, the force on the hard stop will overcome the preload between the second intermediate body and the new grounded body, allowing movement in the new direction. Of course, this strategy could be implemented with various retention mechanisms, though different considerations may be required for each (e.g., the use of pulleys to mediate transitions if using gravitational force retention). See Fig. S9 for examples of this design concept implemented using constant-force and retention handoff mechanisms.

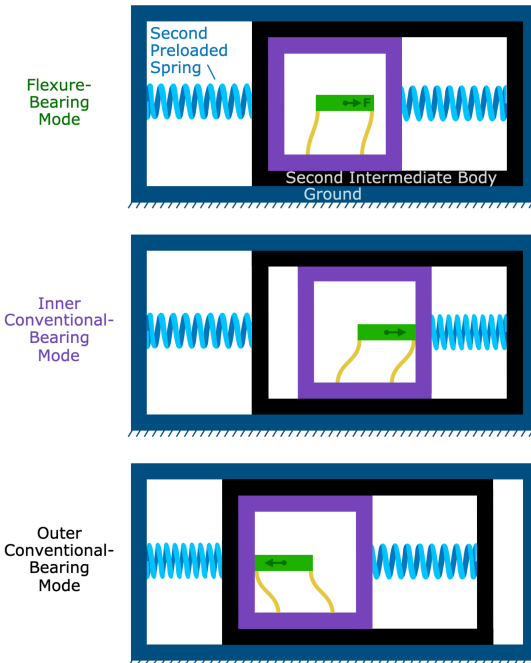


**Fig. 8.** Bidirectional metamorphic flexure bearing (linear force retention). A second conventional bearing enables range extension at both ends of the flexure bearing range of motion. The previously-mechanically-grounded stage becomes a second intermediate body (black) nested within an outer mechanically-grounded stage (dark blue). A second preloaded spring serves as a retention mechanism to hold the second intermediate body against the opposite side of this new grounded body.

In some cases, however, the disadvantages of using a second conventional bearing (e.g., increased part count, increased volume, increased weight) may preclude implementing bidirectional range extension via a second conventional bearing. For such cases, a spring-loaded ball or roller detent [26] may provide the required bidirectional preload while only using a single conventional bearing. Because ball detents are pressed by a preloaded compression spring into a groove with two opposing sloped surfaces, two

evenly balanced preload forces prevent movement in either range extension direction.

To transition a bidirectional metamorphic flexure bearing with ball detents into conventional-bearing mode in either direction, an external force must unbalance these two forces and then overcome the relevant component of the remaining preload on the opposing surface. Hence, a ball detent can ensure that the bearing operates in mutually exclusive modes. We note the complexity introduced in design with the use of a ball detent. Ball detents have conventional bearing properties, along with their disadvantages. And it is also not simple to design a groove geometry that provides a desired force profile for a given application. However, we view the ball detent mechanism as a valuable design candidate for enabling bidirectional motion without the need for an additional motion stage.

### *5.2.3 Rotary Metamorphic Flexure Bearings*

The metamorphic flexure bearing concept generalizes beyond a linear-motion flexure bearing that transforms into a linear-motion conventional bearing. Rather, this concept is a design space that allows a bearing to transition from any set of  $n$  degrees of freedom of compliance to any other set of  $m$  degrees of freedom of sliding or rolling, all while only exerting force between the grounded body and the stage. For instance, this design space enables a mechanical designer to design a single-degree-of-freedom linear-motion flexure bearing with an intermediate body docked to a ground catch that can transition when needed to two degrees of freedom using conventional linear bearings. More simply, though, this design concept allows for rotary metamorphic flexure

bearings. For instance, by nesting a cross-axis flexural pivot [27] inside a conventional rotary bearing and implementing one of the retention mechanisms discussed above, a rotary flexure bearing can transform into a conventional rotary bearing at the end of its range of motion, enabling rotary flexure bearings to be used in applications intermittently requiring substantially higher rotations.

#### *5.2.4 Continuous Repositionability of the Flexure Bearing Range*

Thus far, we have limited our discussion to the use of passive components that enforce position-activated transitions between the bearing's modes. However, one can instead use *active* mechanisms to secure the conventional bearing, allowing the repositioning of the flexure bearing range at any point along the conventional bearing's range. For instance, an active retention mechanism (e.g., a friction brake) that engages at any point along a conventional bearing's range would allow the efficient independent local motion of a flexure bearing at *any* point along the much larger range provided by the intermittently used conventional bearing. Alternatively, some applications may benefit from the use of separate actuators independently driving the flexure and conventional bearings, with the conventional bearing actuator being non-backdriveable to ensure that the flexure-bearing benefits are preserved (in which case, the non-backdriveability of the actuator acts as the retention mechanism). Whether the added cost, size, or complexity of these or other active components are worth the added benefits will vary from one application to another.

### 5.3 Applications

Bearings are used in various applications, from precision manufacturing to automotive and aerospace transportation to medical devices. Bearings that wear in such applications can be costly, dangerous, and time-consuming [28–30]. Metamorphic flexure bearings provide, for applications that typically have a small range of motion but occasionally need range extension, a solution to bearing wear that has the potential to substantially improve the lifetime of such mechanisms. For instance, when using a constant-force retention mechanism, this new bearing concept enables automotive vibration dampening via flexure-based shock absorbers that do not bottom out due to constant-force range extension beyond the range of the flexure bearing. Similarly, the constant-force retention mechanism could improve human safety as a force-based mechanical clutch for human-robot interaction, where large robots transition into a conventional-bearing mode to avoid human injury when a mechanically-programmed force threshold is exceeded.

Metamorphic flexure bearings can also go beyond simply reduction in wear, enabling the use of flexure bearings in applications where a flexure bearing alone would fail under the application's full range of motion. For instance, a rotary metamorphic flexure bearing could be used to design a prosthetic knee [17] with a range and load capacity corresponding to the knee's most typical kinetics (i.e., walking biomechanics), then allow a user to occasionally utilize an extended range of motion (e.g., for sitting, squatting, or kneeling) via a conventional bearing. In the realm of manufacturing, this

class of bearing could instead be used for high-precision applications such as pick-and-place machines [31] or 3D printers, where the high-precision of the bearing in flexure-bearing mode relative to itself is an important parameter, but then conventional-bearing mode can be used for gross manipulation or to clear the build space between builds, or in the case of pharmaceutical manufacturing, to refill supply between the filling of syringes or vials. And the metamorphic flexure bearing concept could be used to design new failure modes for bearings [32,33] – a bearing that typically operates in conventional-bearing mode could fail into a small-range-of-motion compliant mode so that it can remain in service with a reduced range of motion, or a bearing that typically operates in flexure-bearing mode could fail into a conventional-bearing mode if it is overloaded in a direction that is not protected against by force isolation.

This new bearing concept also has the potential to unleash new research directions with respect to mechanisms that transform their mechanical properties over their range. The design space of sequential deformation and motion is a vast playground for mechanism design [34,35], and metamorphic flexure bearings may offer an improvement over sequential metamaterials that are range-limited and would thus benefit from incorporating conventional bearings. In one instance, these bearings are a new foray into kinesthetic force feedback to human operators [36]. For example, an accelerator pedal with force feedback in the form of this new design topology with linear-force retention and a large force step could be used to provide feedback on the redline of a vehicle's engine (e.g., 7,000 RPM) or as the threshold for engaging the vehicle's kinetic

engine recovery system [37]. We thus anticipate numerous applications of the metamorphic flexure bearing and a variety of new technologies that it will enable.

In this work, we have developed the metamorphic flexure bearing concept and designed and characterized a metamorphic flexure bearing prototype using three different retention mechanisms. For design engineers to improve the limits of machine performance, new and improved mechanisms are needed. Having characterized this bearing and extensively discussed its many possible design variables, we conclude that this new class of mechanisms holds great promise for extending machine limits, and we are excited to see its use in various applications, from medical devices to transportation to precision manufacturing.

## **ACKNOWLEDGMENT**

The authors thank Aaron Jaeger, Brandon Peterson, Armin Pomeroy, Antonio Ramirez, Humberto Rosas, Michael Rose, Anthony Singleton, Marcel Thomas, Alyssa Tomkinson, and David Trumper for their helpful advice, suggestions, feedback, and support.

## **FUNDING**

This work was supported by the National Institutes of Health (NIH) New Innovator Award under grant number DP2HD111538.

## CONFLICT OF INTEREST STATEMENT

C.R.T., H.K.L., J.B.H., and T.R.C. are inventors on a patent related to this work. The remaining authors declare that they have no competing interests.

## DATA AVAILABILITY

All data needed to evaluate the conclusions in the paper are freely available at:

<https://doi.org/10.5281/zenodo.15008667>.

## REFERENCES

- [1] Dowson, D., 1998, *History of Tribology*, Professional Engineering Publishing Limited, London and Bury St Edmunds.
- [2] Neale, M. J., 1995, *The Tribology Handbook*, Butterworth-Heinemann.
- [3] Luo, J., Liu, M., and Ma, L., 2021, "Origin of Friction and the New Frictionless Technology—Superlubricity: Advancements and Future Outlook," *Nano Energy*, **86**, p. 106092. <https://doi.org/10.1016/j.nanoen.2021.106092>.
- [4] Meng, Y., Xu, J., Jin, Z., Prakash, B., and Hu, Y., 2020, "A Review of Recent Advances in Tribology," *Friction*, **8**(2), pp. 221–300. <https://doi.org/10.1007/s40544-020-0367-2>.
- [5] Hutchings, I. M., 2016, "Leonardo Da Vinci's Studies of Friction," *Wear*, **360–361**, pp. 51–66. <https://doi.org/10.1016/j.wear.2016.04.019>.
- [6] Jost, H. P. I., 1966, *Lubrication (Tribology) Education and Research, A Report on the Present Position and Industry's Needs*, Her Majesty's Stationery Office, Department of Education and Science, London, UK.
- [7] Howell, L. L., Magleby, S. P., and Olsen, B. M., 2013, *Handbook of Compliant Mechanisms*, Wiley Online Library.
- [8] Hopkins, J. B., and Culpepper, M. L., 2010, "Synthesis of Multi-Degree of Freedom, Parallel Flexure System Concepts via Freedom and Constraint Topology (FACT) – Part I: Principles," *Precision Engineering*, **34**(2), pp. 259–270. <https://doi.org/10.1016/j.precisioneng.2009.06.008>.
- [9] Panas, R. M., and Hopkins, J. B., 2015, "Eliminating Underconstraint in Double Parallelogram Flexure Mechanisms," *Journal of Mechanical Design*, **137**(9), p. 092301. <https://doi.org/10.1115/1.4030773>.
- [10] Merriam, E. G., Lund, J. M., and Howell, L. L., 2016, "Compound Joints: Behavior and Benefits of Flexure Arrays," *Precision Engineering*, **45**, pp. 79–89. <https://doi.org/10.1016/j.precisioneng.2016.01.011>.

- [11] Howell, L. L., 2001, "Introduction," *Compliant Mechanisms*, Wiley.
- [12] Peterson, B. T., Hardin, T. J., Pomeroy, A. W., Hopkins, J. B., and Clites, T. R., 2024, "Cross-Axis Flexural Pivots in Mechatronic Applications: Stress-Based Design for Combined Tension and Bending," *IEEE/ASME Transactions on Mechatronics*, **29**(2), pp. 913–923. <https://doi.org/10.1109/TMECH.2023.3334994>.
- [13] Breńkacz, Ł., Witanowski, Ł., Drosińska-Komor, M., and Szewczuk-Krypa, N., 2021, "Research and Applications of Active Bearings: A State-of-the-Art Review," *Mechanical Systems and Signal Processing*, **151**, p. 107423. <https://doi.org/10.1016/j.ymssp.2020.107423>.
- [14] Trease, B. P., Moon, Y.-M., and Kota, S., 2004, "Design of Large-Displacement Compliant Joints," *Journal of Mechanical Design*, **127**(4), pp. 788–798. <https://doi.org/10.1115/1.1900149>.
- [15] Armentrout, R. W., and Paquette, D. J., 1993, "Rotordynamic Characteristics of Flexure-Pivot Tilting-Pad Journal Bearings," *Tribology Transactions*, **36**(3), pp. 443–451. <https://doi.org/10.1080/10402009308983182>.
- [16] Cannon, J. R., Lusk, C. P., and Howell, L. L., 2008, "Compliant Rolling-Contact Element Mechanisms," American Society of Mechanical Engineers Digital Collection, pp. 3–13. <https://doi.org/10.1115/DETC2005-84073>.
- [17] Zirbel, S., Curtis, S., Bradshaw, R., Duffield, L., Teichert, G., Williams, N., Rorrer, R., Magleby, S., and Howell, L., 2012, "Bi-Behavioral Prosthetic Knee Enabled by a Metamorphic Compliant Mechanism," *Advances in Reconfigurable Mechanisms and Robots I*, J.S. Dai, M. Zoppi, and X. Kong, eds., Springer, London, pp. 401–409. [https://doi.org/10.1007/978-1-4471-4141-9\\_36](https://doi.org/10.1007/978-1-4471-4141-9_36).
- [18] Hooke, R., 1678, *Lectures de Potentia Restitutiva, or of Spring: Explaining the Power of Springing Bodies*, The Royal Society, London.
- [19] Wahl, A. M., 1963, *Mechanical Springs*, McGraw-Hill, New York.
- [20] Wang, C.-Y., and Watson, L., 1980, "Theory of the Constant Force Spring," *Transactions of the ASME*, **47**, pp. 956–958.
- [21] Zampoli, V., and Hetnarski, R. B., 2024, "Constant Force Spring System With a Spiral: Accuracy Assessment," *Journal of Mechanisms and Robotics*, **16**(3), p. 031016.
- [22] Li, M., and Cheng, W., 2018, "Design and Experimental Validation of a Large-Displacement Constant-Force Mechanism," *Journal of Mechanisms and Robotics*, **10**(051007), pp. 1–15. <https://doi.org/10.1115/1.4040437>.
- [23] Nathan, R., 1985, "A Constant Force Generation Mechanism," *Transactions of the ASME*, **107**, pp. 508–512.
- [24] Meng, H., Morgan, J., Wei, Q., and Chen, C., 2018, "Design of Smart Magnetic Devices," *Proceedings of 25th International Workshop on Rare-Earth and Future Permanent Magnets and Their Applications (REPM 2018)*, Beijing, China.
- [25] Jeffries, L., and Lentink, D., 2020, "Design Principles and Function of Mechanical Fasteners in Nature and Technology," *Applied Mechanics Reviews*, **72**(050802), pp. 1–24. <https://doi.org/10.1115/1.4048448>.

- [26] Sclater, N., and Chironis, N. P., 2007, "Latching, Fastening, and Clamping Devices and Mechanisms: Detents for Stopping Mechanical Movements," *Mechanisms and Mechanical Devices Sourcebook*, McGraw-Hill, New York, pp. 246–247.
- [27] Young, W. E., 2021, "An Investigation of the Cross-Spring Pivot," *Journal of Applied Mechanics*, **11**(2), pp. A113–A120. <https://doi.org/10.1115/1.4009358>.
- [28] Kumar, P., Khalid, S., and Kim, H. S., 2023, "Prognostics and Health Management of Rotating Machinery of Industrial Robot with Deep Learning Applications—A Review," *Mathematics*, **11**(13), p. 3008.
- [29] Kumar, N., and Satapathy, R., 2023, "Bearings in Aerospace, Application, Distress, and Life: A Review," *J Fail. Anal. and Preven.*, **23**(3), pp. 915–947. <https://doi.org/10.1007/s11668-023-01658-z>.
- [30] He, C., Wu, Y., and Chen, T., 2019, "Prognostics and Health Management of Life-Supporting Medical Instruments," *J Comb Optim*, **37**(1), pp. 183–195. <https://doi.org/10.1007/s10878-017-0218-x>.
- [31] Zhang, Y., Chen, B. K., Liu, X., and Sun, Y., 2010, "Autonomous Robotic Pick-and-Place of Microobjects," *IEEE Transactions on Robotics*, **26**(1), pp. 200–207. <https://doi.org/10.1109/TRO.2009.2034831>.
- [32] Xu, F., Ding, N., Li, N., Liu, L., Hou, N., Xu, N., Guo, W., Tian, L., Xu, H., Lawrence Wu, C.-M., Wu, X., and Chen, X., 2023, "A Review of Bearing Failure Modes, Mechanisms and Causes," *Engineering Failure Analysis*, **152**, p. 107518. <https://doi.org/10.1016/j.engfailanal.2023.107518>.
- [33] Fowler, R. M., Howell, L. L., and Magleby, S. P., 2011, "Compliant Space Mechanisms: A New Frontier for Compliant Mechanisms," *Mechanical Sciences*, **2**(2), pp. 205–215. <https://doi.org/10.5194/ms-2-205-2011>.
- [34] Bertoldi, K., Vitelli, V., Christensen, J., and van Hecke, M., 2017, "Flexible Mechanical Metamaterials," *Nat Rev Mater*, **2**(11), pp. 1–11. <https://doi.org/10.1038/natrevmats.2017.66>.
- [35] Farzaneh, A., Pawar, N., Portela, C. M., and Hopkins, J. B., 2022, "Sequential Metamaterials with Alternating Poisson's Ratios," *Nat Commun*, **13**(1), p. 1041. <https://doi.org/10.1038/s41467-022-28696-9>.
- [36] Giri, G. S., Maddahi, Y., and Zareinia, K., 2021, "An Application-Based Review of Haptics Technology," *Robotics*, **10**(1), p. 29. <https://doi.org/10.3390/robotics10010029>.
- [37] Cross, D., and Hilton, J., 2008, "High Speed Flywheel Based Hybrid Systems for Low Carbon Vehicles," *IET HEVC 2008 - Hybrid and Eco-Friendly Vehicle Conference*, pp. 1–5. <https://doi.org/10.1049/cp:20081062>.

# Supplementary Materials for

## Metamorphic Flexure Bearings for Extended Range of Motion

Cameron R. Taylor *et al.*

\*Address correspondence to: Cameron R. Taylor; [ctaylor7@unc.edu](mailto:ctaylor7@unc.edu) and Tyler R. Clites; [clites@ucla.edu](mailto:clites@ucla.edu).

**This supplementary information includes:**

Glossary  
Figs. S1-S9  
Sections S1-S4  
Thumbnails for Movies S1-S2

## Glossary

**Metamorphic Flexure Bearing** A bearing that mediates movement via a flexure bearing during standard operation, but automatically transitions to the use of a conventional bearing as needed for further range of motion

- **Stage** Primary moving component, the position of which always corresponds directly to the bearing's position
- **Intermediate Body** Component that only moves when range extension is needed
- **Grounded Body** Fixed component of the bearing (also referred to as simply "ground")

**Mode** The current operational configuration of the bearing, defined by which of the internal bearings is active

- **Flexure-Bearing Mode** Mode in which all movement directly corresponds to flexure-bearing movement
- **Conventional-Bearing Mode** Mode in which all movement directly corresponds to conventional-bearing movement
- **Transition** Brief period during which the mechanism is between flexure-bearing and conventional-bearing mode
  - **Stage Attachment** Attachment of the stage to the intermediate body (typically occurring at the start of transition during lengthening)
  - **Ground Detachment** Detachment of the intermediate body from ground (typically occurring at the end of transition during lengthening)
  - **Ground Reattachment** Attachment of the intermediate body to ground (typically occurring at the start of transition during shortening)
  - **Stage Detachment** Detachment of the stage from the intermediate body (typically occurring at the end of transition during shortening)
- **Combined Mode** Mode where neither the flexure bearing nor conventional bearing are prevented from moving, resulting from ground detachment without stage attachment or stage detachment without ground reattachment

**Retention Mechanism** Mechanism that exerts force as needed to hold (i.e., retain) two components together as needed

- **Continuous Retention** Retention mechanism strategy that exerts internal negative force on the intermediate body in both flexure-bearing and conventional-bearing modes (e.g., linear-force retention, constant-force retention)
  - **Linear-Force Retention** Retention mechanism strategy that exerts a negative force on the intermediate body in flexure-bearing mode that grows linearly throughout conventional-bearing mode

- **Constant-Force Retention** Retention mechanism strategy that exerts a constant negative force on the intermediate body in flexure-bearing mode that is maintained throughout conventional-bearing mode
    - **Gravitational Retention** Retention utilizing gravitational force on the intermediate body
- **Retention Handoff** Retention mechanism strategy in which two physically-distinct retention mechanisms are used – a ground catch to hold the intermediate body against the grounded body in flexure-bearing mode, and a stage catch to hold the intermediate body against the stage in conventional-bearing mode
  - **Ground Catch** Retention mechanism that exerts force between the intermediate and grounded bodies to maintain contact between them
  - **Stage Catch** Retention mechanism that exerts force between the intermediate body and the stage to maintain contact between them
  - **Conditional Retention** Retention mechanism setup in which the intermediate body is anchored to the grounded body during flexure-bearing mode but *not* anchored to the stage during conventional-bearing mode (i.e., use of a ground catch but no stage catch)
- **Active Retention** Use of an active retention mechanism, such as a friction brake, to secure the conventional bearing portion of the bearing and at any location, and thus achieve continuous repositionability of the flexure bearing range

**Force Profile** The force required to quasi-statically actuate (slowly move) or steadily hold a metamorphic flexure bearing at a given position in its range of motion

- **Home Position** Location of the stage (relative to the grounded body) when the intermediate body is anchored to the grounded body and the flexure bearing is at its zero-force point
- **Home Side** Positioned towards the side of the bearing that has the ground-side grip-fixture
- **Far Side** Positioned towards the side of the bearing that has the stage-side stage grip fixture

## S1 Design and Assembly Details

For the conventional bearing, we printed the intermediate body on a Markforged Mark Two in Onyx filament (micro carbon fiber filled nylon), then press fit and bolted in the two square-profile plain bearings (igus QJRMP-01-10) end-to-end within the intermediate body (see the cross-section of Fig. 2). We then slid the press-fit linear-motion bearings onto a 150-mm-long, 7.5-mm-wide square profile shaft (Igus AWMQ-10), which served as the main chassis for the grounded body. We used a 165-mm-long bolt (McMaster-Carr [McM-C] 90044A262) through the base shaft to secure both ends of the grounded body (also printed on the Mark Two) onto the shaft, tightening the bolt (only lightly, to minimize shaft deflection) into a square nut (McM-C 94785A411) that we press fitted into the home side (left side of figure) of the grounded body.

For the flexure bearing, we designed the flexures along with their rigid bars and attachment rings as a single continuous component (see the detailed view at top center of Fig. 2). We printed this flexure component on an UltiMaker S5 in UltiMaker Tough PLA filament (poly[lactic acid] mixed with acrylic polymer, with a Young's modulus of 2.8 GPa and a tensile stress at yield of 45 MPa), using UltiMaker Breakaway (polylactic acid mixed with thermoplastic polyurethane) as a support material. The flexures were 600  $\mu\text{m}$  thick and were printed in four 150  $\mu\text{m}$  layers in the X-Y plane. We then printed the far-side of the intermediate body (constituting the flexure bearing far-side internal hard stop) on a Bambu Lab X1C in PLA-CF (carbon fiber reinforced PLA) and the stage extension with the same printer and material as the flexure component. Using thin M3 nuts (McM-C 93935A320) and M3 bolts of various lengths (e.g., McM-C 92290A111), we first affixed the flexure component to the home side of the intermediate body, then affixed the far side of the intermediate body to the far side of the main body of the intermediate body, and finally attached the stage extension to the far side of the stage.

### S1.1 Linear-Force Retention Design

We used three compression springs (McM-C 9657K419, 9657K432, 9657K449) of varying lengths to demonstrate the linear-force retention concept. These springs were composed of zinc-plated music-wire-steel and had identical inner and outer diameters (13 mm ID, 15.2 mm OD) but varied in their resting and maximum compression lengths (resting/minimum lengths: 63.5/13.5 mm, 76.2/15.7 mm, and 88.9/18.0 mm, respectively) and spring rates (0.665 N/mm, 0.543 N/mm, and 0.473 N/mm, respectively).

To insert or swap the compression spring, we removed the stage extension, the far side of the intermediate body, and the mechanism-length bolt and far-side grounded-body hard stop. We then slid the new compression spring onto the conventional-bearing shaft and replaced all removed components (see Fig. S1 below). We designed the nominal initial compression to have a 61.45 mm length. As needed, we added 2.58-mm-thickness washers in series with the compression spring to tune the initial preload of the spring. Swapping the compression spring

for springs of different lengths and spring rates and tuning the initial compression of the springs enabled us to achieve various initial preload force levels.

### S1.2 Constant-Force Retention Design

To demonstrate the constant-force-spring retention concept, we incorporated twelve constant-force (c-f) springs into the home side of the grounded body. Each c-f spring (McM-C 9293K122) maintained a constant force of 1.02 N and was sized (13.5 mm ID, 15.7 mm OD, 6.35 mm width) to hold itself with some compressive force around a ball bearing (igus B605B3E, 5 mm ID, 14 mm OD, 5 mm width) mounted to one of twelve bolt slots in the grounded body via an M5 threaded rod (McM-C 93805A286) and two thin hex nuts (McM-C 90710A037). To mount each c-f spring onto a ball bearing, we extended the c-f spring to near full extension to render its inner ring compliant, then seated this inner ring on the outside of the bearing (see Fig. S2 below).

To tune the force of the constant-force retention, we attached the number of parallel c-f springs required to achieve a given force. To avoid unnecessarily adding an internal torque to the bearing, we attached the twelve c-f springs in radially opposite pairs, giving a total of six different force levels to test (2, 4, 6, 8, 10, and 12 springs).

### S1.3 Retention Handoff Design

We custom-designed tunable magnetic catches to demonstrate the retention handoff concept (see Fig. 2 bottom center) using steel magnetic-flux-directing components extracted from standard off-the-shelf magnetic latches (Everbilt 9235997). We began the assembly of each catch by placing one steel plate on a work surface. Using a 3D-printed support structure (printed on the Mark Two) with a pattern of low-tolerance slots for magnets, we used a colored bar magnet as a manual pick-and-place tool to insert a variable number of rectangular permanent magnets (3 mm long, 2 mm wide, 1 mm thick, grade N50, nickel-plated, and magnetized through their thickness [SuperMagnetMan M0301]) onto the first steel plate, north-poles up. To tune the size of the magnetic-catch force, we placed only as many magnets as needed to provide the desired force. To make the force tuning scale roughly linearly with the number of magnets, we designed the catch to accommodate magnets in parallel (as opposed to stacking them in series). After placing the magnets, we used magnetic viewing film to ensure that all magnets were oriented in the same direction by visually checking that the magnetic field strength above the magnets was convex (see Fig. S3 below). Then, maintaining the 3D-printed support structure in place, we slid the second steel plate onto the north-pole side of the magnets. We designed the support structure to be thinner than the magnets, so once the catch was assembled, all magnets had contact with both steel plates. We then clipped a clothespin-style retainer over the back of the magnetic catch, pressing the steel plates as far forward inside the support structure as possible, ensuring that the steel plates would extend out of the catch a repeatable distance. Finally, we inserted a magnetic catch into the grounded body (see Fig. S4 below) and a magnetic catch into the intermediate body. To prevent movement of the catches relative to their respective rigid bodies, we affixed them into place using M3 set screws

through the bodies of their respective rigid bodies. We repeated this assembly process each time we needed to tune the force. The steel armatures were permanently affixed at their corresponding locations using 3/8 inch #4 zinc Phillips flat-head wood screws, which we tightened until their heads did not protrude further than the extension of the 1.55-mm-thick steel plates from the catch. Though we originally designed two slots for each of the catches, we only used one slot for each to maximize the repeatability of the transitions.

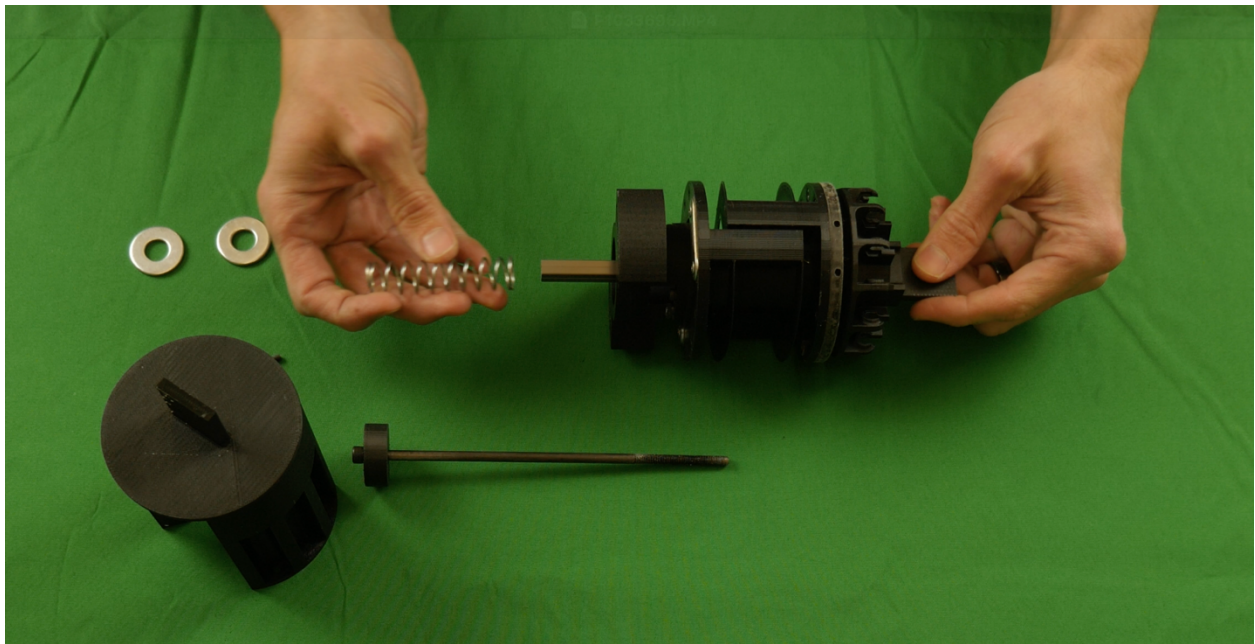


**Fig. S1.** Compression Spring Assembly. This photograph demonstrates insertion of the compression spring onto the conventional-bearing shaft. We used washers (shown at top left) to adjust the compression spring's preload.



**Fig. S2.** Constant-Force Spring Assembly. This photograph demonstrates extension of the c-f spring and seating of its inner ring on the outside of a ball bearing. The bolt and nuts used to attach the c-f spring to the grounded body are shown at right.

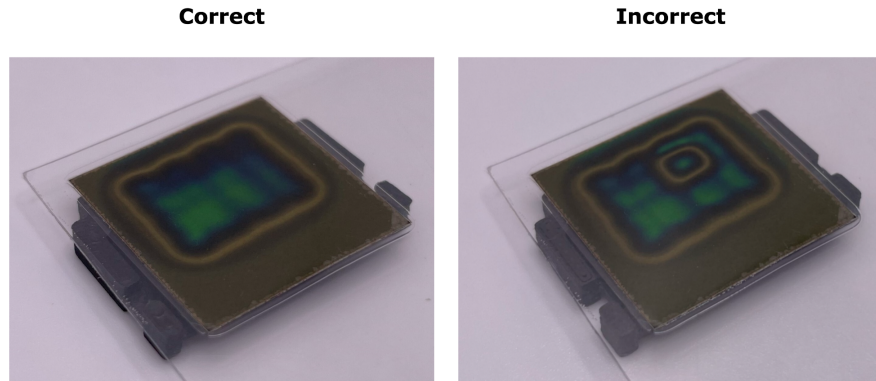


**Fig. S3.** Verification of magnet alignment using magnetic viewing film. When all permanent magnets are aligned in the same direction, one contour is seen in the magnetic viewing film (figure on left). In contrast, multiple contours appear when any magnet is reversed relative to the others (figure on right). Thus, these multiple contours can be used as an indication that the magnetic catch was incorrectly assembled. This verification method only works when the top steel plate is removed (when the magnetic catch has not yet been fully assembled).

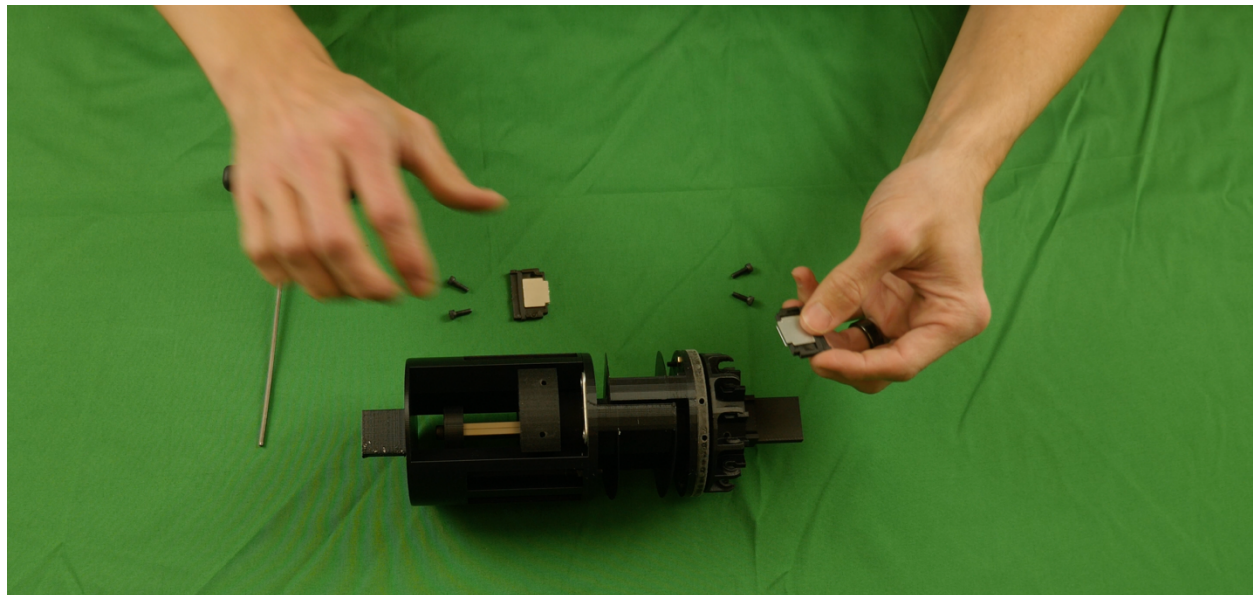


**Fig. S4.** Magnetic Catch Assembly. This photograph demonstrates insertion of a magnetic catch into the grounded body. The pairs of set screws we used to secure the magnetic catches are also shown next to each magnetic catch.

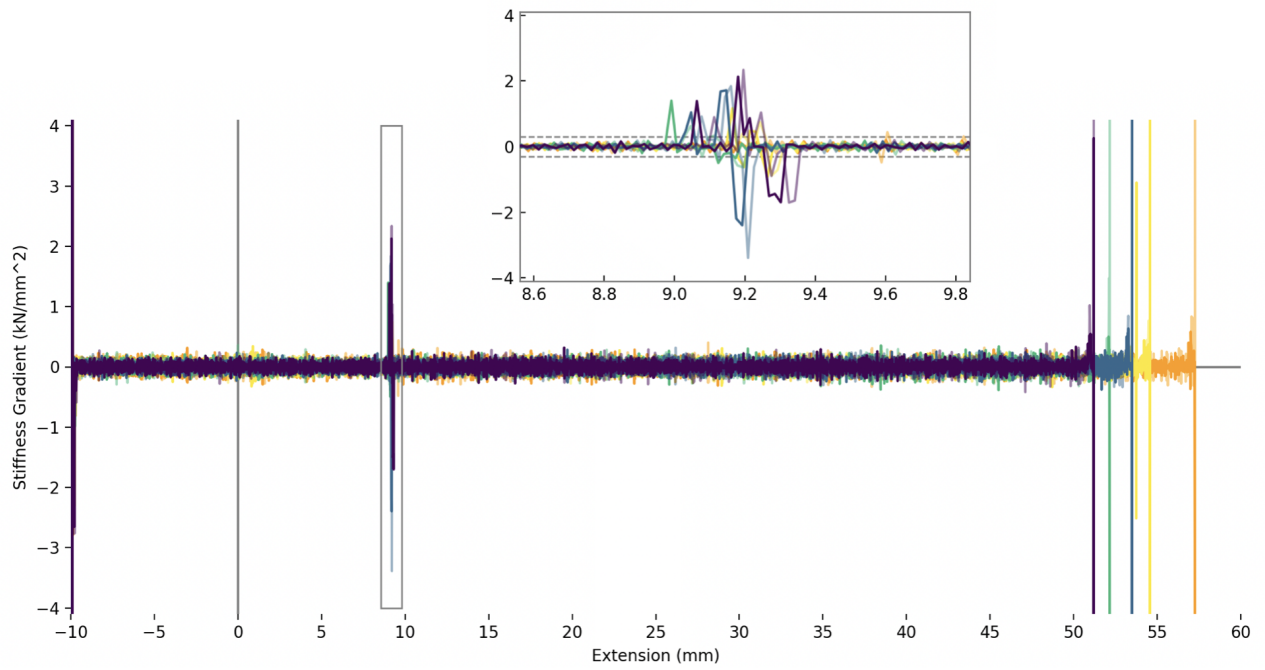


**Fig. S5.** Bearing Stiffness Gradient with Linear-Force Retention. This plot shows the stiffness gradient versus extension for the linear-force retention case. We used the stiffness gradient to determine transition locations.

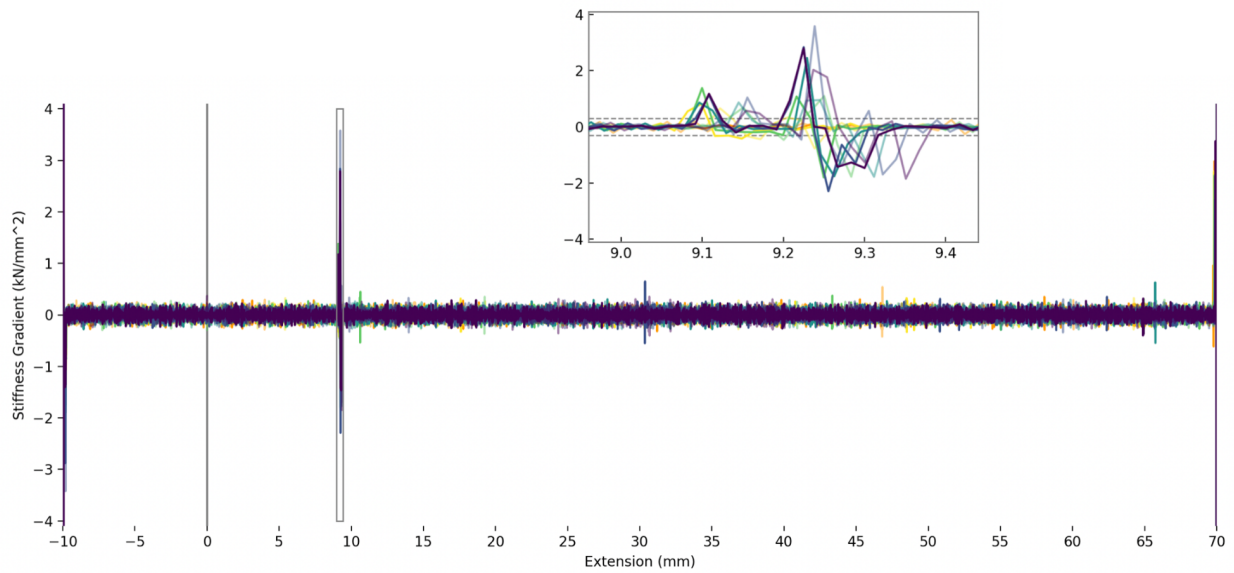


**Fig. S6.** Bearing Stiffness Gradient with Constant-Force Retention. This plot shows the stiffness gradient versus extension for the constant-force retention case. We used the stiffness gradient to determine transition locations.

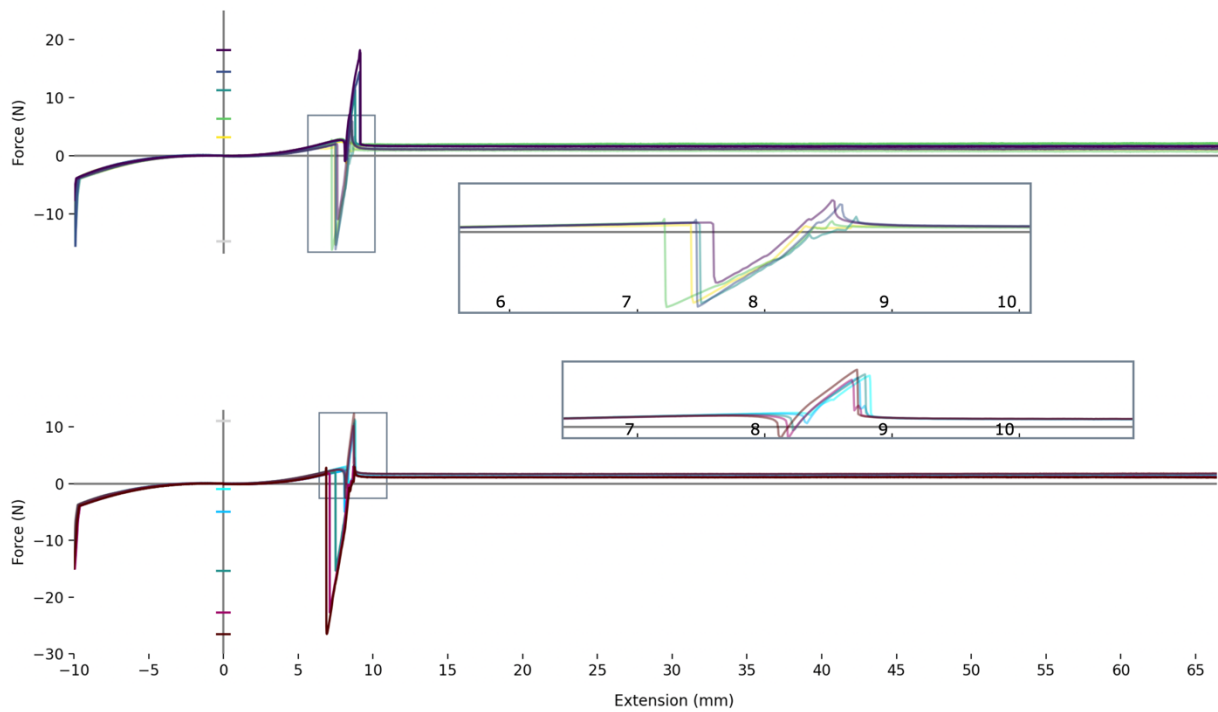


**Fig. S7.** Alternative Sweep Zoom Insets. Fig. 7 in the main body of the paper shows the ground and stage preloads as they are swept. This figure here instead shows zoomed-in views of the attachment forces as the corresponding preloads are being swept. In the top plot, this corresponds to the transition on the shortening curves, and on the bottom plot, this corresponds to the lengthening curves. For consistency with the main paper figure, curves of interest for this figure are shown with an alpha value of 0.5.

## **Section S2 Grounded Body Acceleration**

The discussion in the paper about the maximum negative acceleration of the metamorphic flexure bearing applies only to the intermediate body's acceleration relative to the global frame. In conventional-bearing mode, if the stage is kept fixed and the grounded body is accelerated, acceleration of the intermediate body mass is no longer a factor and only friction must be accounted for. Similarly, if both the grounded body and stage are accelerated relative to the global frame, it is the true acceleration of the intermediate body relative to the global frame that matters. For instance, if *both* the ground and the stage are negatively accelerated, even if the metamorphic flexure bearing does not change length, this scenario can also switch the bearing into combined mode. Further, when in flexure-bearing mode, “grounded” body negative acceleration can result in a transition to a combined mode if the ground-catch force is insufficient to accelerate the intermediate body mass.

### Section S3 Magnetic Catch Asymmetry Model

Note the setup illustrated in Fig. S8 below. Let the force between the steel plate and the magnet be governed by  $F = c / d^a$ , where  $d$  is the distance between the magnet's center and the steel plate's center and  $a$  and  $c$  are non-zero positive constants. Further, let the compliant component have a constant stiffness with a spring constant of  $k$ . The force required for the magnet to extend the spring and attach to the steel, then, is  $F = kx$ , where  $x$  is the position of the steel relative to the ideal attachment point. For the force between the steel plate and the magnet to match the force required to attach the magnet to the steel, then the steel plate must be moved to or closer than the attachment point  $x_{\text{attachment}} = c / (kd^a)$ . Thus, there is some non-zero distance  $d$  between the steel and magnet on approach where the force becomes sufficient to extend the spring and the magnet rapidly crosses that distance to attach to the steel.

On retreat, however, the force between the magnet and the steel is a constant,  $F_{\max}$ , so the magnet and steel separate at  $x_{\text{separation}} = F_{\max} / k$ .

Note that with infinite stiffness  $k$ , the actual attachment and separation points are the ideal attachment and separation points  $x = 0$ , and that both the actual attachment and separation locations grow with decreasing stiffness. For a non-zero positive  $k$ , it can also be shown that  $x_{\text{attachment}}$  increases with increasing  $c$  (increasing the magnetic catch strength increases attachment distance) and that  $x_{\text{attachment}}$  decreases with increasing  $a$  (localizing the magnetic catch force [so that the force occurs closer to contact] reduces attachment distance).

This example illustrates that compliance in rigid components alters attachment and separation points and forces for catches. Because the various possible types of retention mechanisms used for retention handoff will have different force profiles than a magnetic catch, the profile of each should be considered when considering the implications of rigid component compliance. Further, rigid component compliance can have effects on continuous retention mechanisms as well that should be considered in design.

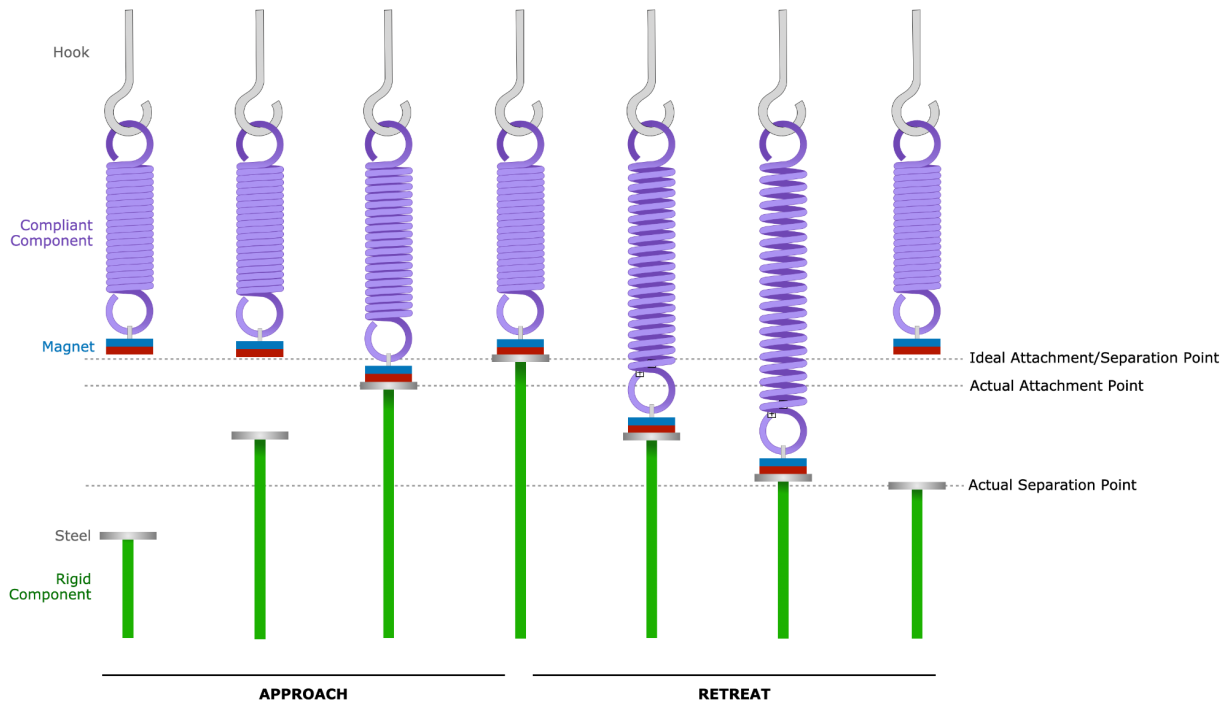


**Fig. S8. Magnetic Catch Asymmetry.** This diagram visually highlights the phenomenon resulting in asymmetry between the magnetic catch attachment and separation forces and locations. A compliant component (purple) hangs from a mechanically-grounded hook and has a magnet attached to its lower end. The magnet is approached by a ferromagnetic steel plate (gray) affixed to the top of a rigid component (green). On approach, the magnet only attaches to the steel when it draws close, which slightly stretches the compliant component, and the rigid component experiences a force equal only to the compliant component's stretch times its stiffness. On retreat, however, because the magnet and steel are already attached, the full contact force is exerted internally between the two elements as a preload, and the compliant component stretches until it exerts a force sufficient to overcome this preload. Thus, when one (or both) of the components containing magnetic catch elements are compliant, they experience a reduced attachment force at a slight offset on approach and a full detachment force at a larger offset on retreat.

## **Section S4 Further Exploration of Possible Retention Mechanisms**

While an encyclopedic listing of possible retention mechanisms would be unnecessary, a moderate exploration into possibilities informs an understanding of the bearing's operation. Thus, we here note a variety of retention mechanism configurations and the implications of their use.

### **S4.1 Continuous Retention Mechanisms**

We demonstrated two possible continuous retention mechanisms here: a linear-force retention mechanism and a constant-force retention mechanism. We used a compression spring to implement linear force retention, but an extension spring could similarly be used (consider the "constant-force retention" diagram of Fig. 1, but with the c-f spring replaced with a preloaded extension coil spring). In either case, a spring-like element such as a pneumatic cylinder could be used instead, or a different spring geometry could be used. Further, the same compliant mechanism topology used for the flexure bearing could also be used for the retention mechanism, though the benefits of doing so are not immediately apparent, noting that the metamorphic flexure bearing's advantage lies in its range of motion extension, and thus any spring used for a retention mechanism ought to have a larger range of motion than its corresponding flexure bearing, a requirement that is easier to attain using a compliant mechanism with more degrees of freedom which are then constrained by the conventional bearing. Of course, the force profiles need not be limited to linear or constant force, but can vary in position as needed for a given design. Further, active retention, such as a motorized winch, could provide continuous retention with a force that varies through not only space but time as well.

### **S4.2 Gravitational Retention**

As discussed in the paper, the mass of the intermediate body is an important consideration in retention mechanism design. More intriguing, however, is that gravitational force can *itself* be used as a continuous (specifically, constant-force) retention mechanism.

When doing so, the use of a larger intermediate body mass will allow for greater negative acceleration due to the greater proportion of the force being used to accelerate the mass as opposed to keeping the flexure bearing extended. However, because the mass must always increase to increase the gravitational retention force, the maximum negative acceleration of an intermediate body using gravitational force as a retention mechanism is always limited to the standard gravity of whichever celestial body on which the bearing is operated (e.g., 9.8 m/s<sup>2</sup> on earth).

### **S4.3 Retention Handoff Mechanisms**

Retention handoff differs from continuous retention in that it requires not one but two retention mechanisms that can each attach and detach as needed for transition of the bearing between modes.

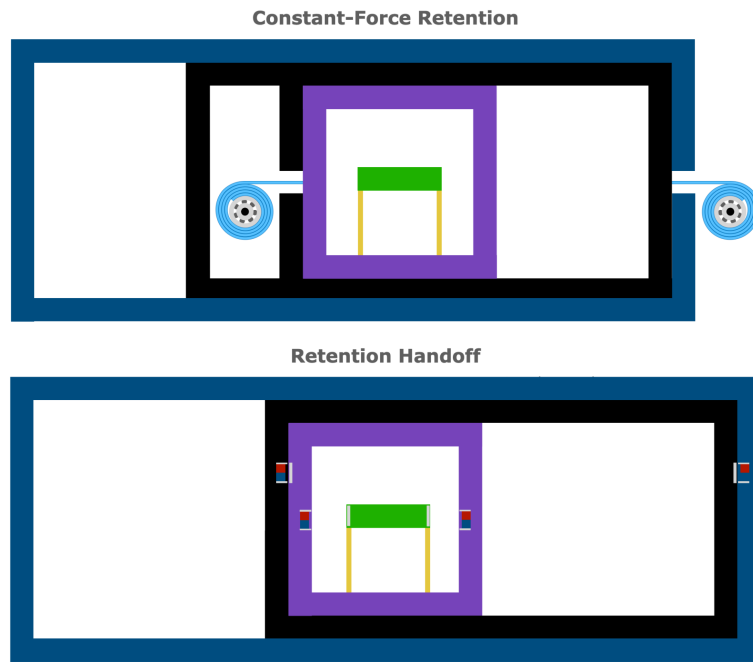
We chose to use magnetic retention in this work because we were interested in exploring its advantages and disadvantages. Magnets are advantageous because they do not require direct contact, and depending on the type of magnetic catch design used, the rigid bodies can even be part of the magnetic circuit. For instance, in the case of the standard magnetic catch design we employed here, the magnet(s) and pair of steel plates could be embedded in a plastic rigid body that is attracted to a steel rigid body. These advantages extend to other magnetic retention strategies. For instance, the retention can be magnet-to-armature (without additional magnetic-flux-directing steel plates) or magnet-to-magnet, and the magnets used can be a single magnet, alternating magnets, a Halbach array, a configuration that repels before it attracts, and so on. Further, all magnetic retention strategies can be tuned (both in maximum force and in the force-position profile) by changing the number or strength of magnets, by tuning the distance (“air” gap) between the magnetic components at contact, or by modifying other aspects of the catch’s geometry. All magnetic retention strategies also share the disadvantages described above of having differences in the force levels and locations of attachment and detachment when the rigid bodies exhibit some compliance. Further, magnetic retention may have a heightened potential for noise generation versus the other strategies we demonstrated here, which is especially difficult to control if they are attached to rigid components exhibiting some compliance. For noise reduction in general, at the cost of greater complexity, compliant or viscoelastic bumpers (possibly with stress relaxation under steady state force) which cushion the force impact or impulse may be considered. While we specifically designed our magnetic catches here to have force profiles with the force concentrated as close to the catch contact as possible, it is a valuable area of further investigation to determine how different force profiles (e.g., larger magnets with a larger air gap at contact for a more linear force profile) affect the noise and controllability of the bearing.

Of course, retention handoff need not include the use of magnets. Spring-loaded mechanisms such as roller catches, ball detents, and snap buttons similarly provide a holding force that resists any movement up to a particular preload, though with a different force profile, which first resists and then assists movement in the process of engaging and which again first resists and then assists movement in the process of disengaging. Touch fasteners, such as Velcro hook-and-loop fasteners or the stem-and-cap fasteners used in 3M Command picture-hanging strips, provide yet another different force profile, requiring only force toward the fastener when engaging and force away from the fastener when disengaging but may provide less repeatable forces than roller or magnetic catches would. And many other possible mechanisms could be implemented as needed for a given design, such as low-tack pressure-sensitive adhesion (e.g., Post-It Note adhesive), suction cups, surface combinations with high static but low kinetic friction (whether naturally occurring or mediated by the inclusion of a lateral magnetic catch), or active mechanisms such as electrostatic or electromagnetic mechanisms, pin locks, or

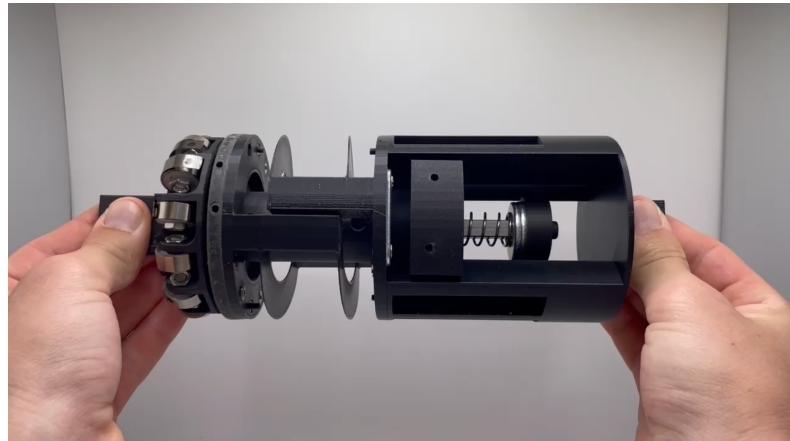
mechanical jaws that can clutch the intermediate body to the grounded body at any desired location. Where needed for a given design, one retention mechanism can even hand off at transition to a retention mechanism of a fully distinct modality. It should be noted that, as noted above in Section S2 Magnetic Catch Asymmetry Model, special considerations should be taken to account for rigid element compliance specific to the different types of retention handoff mechanism noted here.

#### ***S4.4 Conditional Retention***

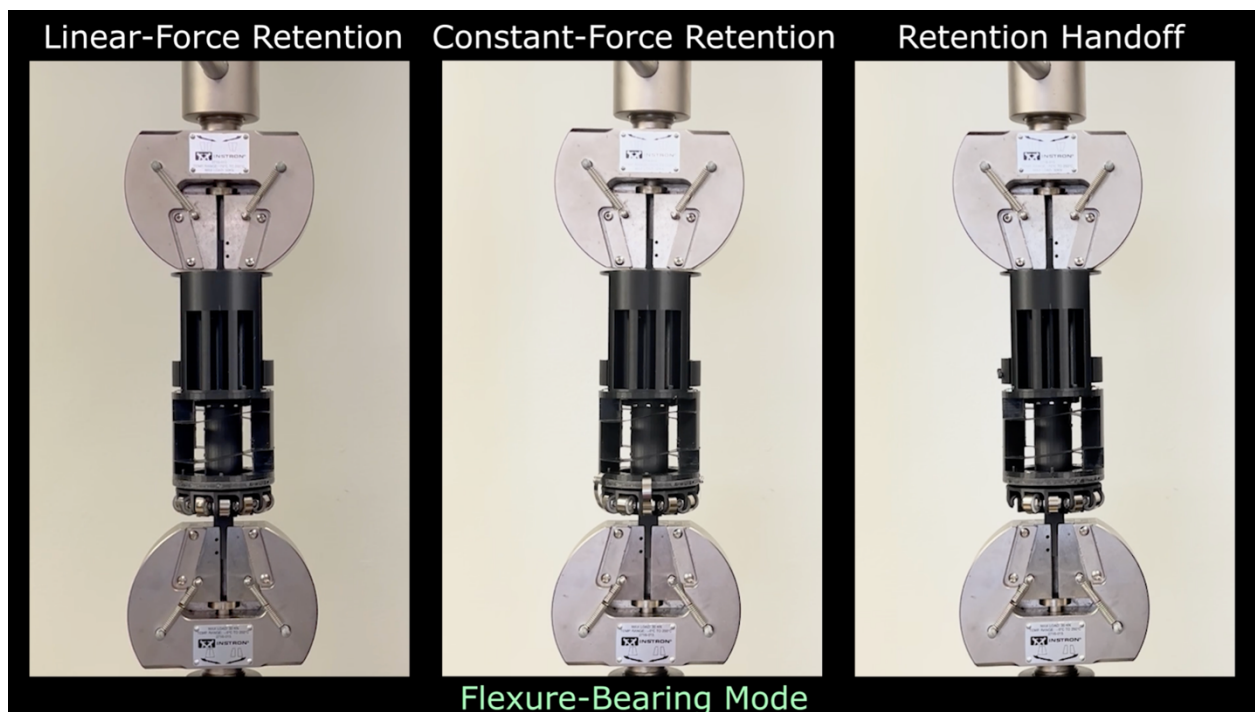
Finally, for designs where a combined mode is acceptable, a conditional retention strategy can be implemented wherein only a single force-detachable retention mechanism – the ground catch – is used, resulting in the bearing having only flexure-bearing and combined modes. The disadvantages of such a strategy (as discussed in the discussion section regarding combined mode with retention handoff) are oscillation of the intermediate body mass at transition and increased conventional-bearing travel before transitioning back to flexure-bearing mode. However, the conditional retention strategy has the advantage of needing only a single catch while still exhibiting unlimited range extension (similar to that provided by the retention handoff strategy), which might be a sufficient advantage in some designs to warrant its implementation. Where relevant, the disadvantage of intermediate-body oscillation in conditional retention can be mitigated by submerging the bearing in an aqueous, viscous, or pneumatic environment to dampen the oscillation, and the disadvantage of a shifted flexure-bearing-mode re-entry transition setpoint is minimized if the bearing typically crosses past its home position after flexure-bearing range re-entry or if it very infrequently enters conventional-bearing mode.



**Fig. S9.** Implementations of a bidirectional flexure bearing using alternative retention mechanisms. Note that in the retention handoff case, the far-side ground catch must have a greater retention force than the far-side stage catch for the mechanism to successfully transition from inner conventional-bearing to flexure-bearing mode (detaching the stage catch) instead of transitioning directly to outer conventional-bearing mode when shortening.



**Movie S1.** Metamorphic Flexure Bearing Demonstration (Linear-Force Retention). For a demonstration of the metamorphic flexure bearing being actuated by hand, see Movie\_S1. The bearing is held in the Movie so that the compression-spring retention mechanism is clearly visible. In this Movie, we actuate the bearing through three cycles of flexure-bearing mode, then actuate the bearing through the length of its conventional-bearing mode before returning it to its home position. Link to supplementary data, code, and videos:  
<https://doi.org/10.5281/zenodo.15008667>.



**Movie S2.** Metamorphic Flexure Bearing Characterization. For a Movie showing an example characterization with each type of retention mechanism, see Movie\_S2. Link to supplementary data, code, and videos:  
<https://doi.org/10.5281/zenodo.15008667>.